



Published in final edited form as:

*Cell Mol Life Sci.* 2012 June ; 69(11): 1855–1873. doi:10.1007/s00018-011-0901-5.

## GEP Constitutes a Negative Feedback Loop with MyoD and Acts as a Novel Mediator in Controlling Skeletal Muscle Differentiation

Dawei Wang<sup>\*.S.†</sup>, Xiaohui Bai<sup>\*.€.†</sup>, Qingyun Tian<sup>\*.†</sup>, Yongjie Lai<sup>\*</sup>, Edward A. Lin<sup>\*</sup>, Yongxiang Shi<sup>\*</sup>, Xiaodong Mu<sup>‡</sup>, Jian Q. Feng<sup>#</sup>, Cathy S. Carlson<sup>£</sup>, and Chuan-ju Liu<sup>\*.‡.¶</sup>

<sup>\*</sup>Department of Orthopaedic Surgery, New York University Medical Center, New York, NY, 10003

<sup>§</sup>Department of Orthopedics, Provincial Hospital Affiliated to Shandong University, Jinan 250021, China

<sup>€</sup>Department of Otorhinolaryngology Head and Neck Surgery, Provincial Hospital affiliated to Shandong University, Jinan 250021, China

<sup>‡</sup>Stem Cell Research Center, Children's Hospital of Pittsburgh and Department of Orthopaedic Surgery, University of Pittsburgh, Pittsburgh, PA 15219

<sup>#</sup>Baylor College of Dentistry, Texas A&M Health Science Center, Dallas, TX 75246

<sup>£</sup>College of Veterinary Medicine, University of Minnesota, St. Paul, MN 55108

<sup>‡</sup>Department of Cell Biology, New York University School of Medicine, New York, NY 10016

### Abstract

Granulin-epithelin precursor (GEP) is an autocrine growth factor that has been implicated in embryonic development, tissue repair, tumorigenesis, and inflammation. Here we report that GEP was expressed in skeletal muscle tissue and its level was differentially altered in the course of C2C12 myoblast fusion. The GEP expression during myoblast fusion was a consequence of MyoD transcription factor binding to several E-box (CANNTG) sequences in the 5'-flanking regulatory region of GEP gene, followed by transcription. Recombinant GEP potently inhibited myotube formation from C2C12 myoblasts whereas the knockdown of endogenous GEP via a siRNA approach accelerated the fusion of myoblasts to myotubes. Interestingly, the muscle fibers of GEP knockdown mice were larger in number but noticeably smaller in size when compared to wild-type. Mechanistic studies revealed that during myoblast fusion, the addition of GEP led to remarkable reductions in the expressions of muscle-specific transcription factors, including MyoD. In addition, the regulation of myotube formation by GEP is mediated by the anti-myogenic factor JunB, which is upregulated following GEP stimulation. Thus, GEP growth factor, JunB, and MyoD transcription factor form a regulatory loop and act in concert in the course of myogenesis.

### INTRODUCTION

Granulin-epithelin precursor (GEP), also referred to as progranulin, proepithelin, PC cell derived growth factor, or acrogranin, is a secreted growth factor (3, 6, 47, 55, 76). GEP is heavily glycosylated and appears as a ~90-kDa protein on SDS-PAGE. GEP is secreted in an intact form (66, 76) and undergoes proteolysis, leading to the release of its constituent

<sup>¶</sup>To whom correspondence should be addressed: Chuan-Ju Liu, PhD, Department of Orthopaedic Surgery, New York University School of Medicine, 301 East 17th Street, New York, NY 10003. Tel: 212-598-6103; Fax: 212-598-6096; chuanju.liu@nyumc.org.

<sup>†</sup>These authors contribute equally to the paper.

peptides, the granulins (14, 38, 73). GEP is abundantly expressed in rapidly cycling epithelial cells, in cells of the immune system, in neurons, and in chondrocytes (1, 3, 13, 19, 21, 38, 67). High levels of GEP expression have been reported in several human cancers, and GEP is believed to contribute to the tumorigenesis of breast cancer, clear cell renal carcinoma, invasive ovarian carcinoma, glioblastoma, adipocytic teratoma, multiple myeloma, and osteosarcoma (5, 14, 20, 23–25, 63, 74). The role of GEP in the regulation of cellular proliferation has been well characterized. Mouse embryo fibroblasts derived from mice with a targeted deletion of the insulin-like growth factor receptor gene ( $R^{-}$  cells) are unable to proliferate in response to insulin-like growth factor and other growth factors (EGF and platelet-derived growth factor) that are necessary for cell cycle progression (54). In contrast, GEP allows the cell to bypass the requirement for the insulin-like growth factor receptor, thus promoting the growth of  $R^{-}$  cells (68, 73). Increasing evidence has implicated GEP in a number of important biological functions. GEP has been isolated as a differentially expressed gene in mesothelial differentiation (58), sexual differentiation of the brain (59), and macrophage development (4). GEP is a crucial mediator of wound healing and tissue repair (24, 77). GEP is also found in the synovium of rheumatoid arthritis and osteoarthritis patients (26). Recently, GEP has been found to directly bind to TNF receptors and play an important role in inflammatory arthritis (35, 36, 61). Although GEP has been shown to be a key downstream molecule of BMP2 in the course of chondrogenesis by activating Erk1/2 signaling and JunB transcription factor (19, 21, 34), its role in skeletal muscle tissue has yet to be investigated.

The development of skeletal muscle requires a host of transcription factors that lead the cell toward the path of myogenic differentiation. These “myogenic factors” include MyoD (15), Myf5 (8), myogenin (16, 62), and MRF4 (49, 66). The overexpression of myogenic factors in some non-myogenic cell types, such as C3H10T1/2 fibroblasts, can result in the activation of various muscle differentiation genes. In some cases, this can lead to the fusion of myoblasts to form myotubes, one of the hallmark events of muscle differentiation (2, 12, 15, 52). Differentiation of skeletal muscle requires the irreversible withdrawal of the myoblast from the cell cycle (31, 44, 50). The HLH domains of MyoD mediate homodimerization, or heterodimerization with another class of HLH proteins, such as E12/E47 (15, 16, 30), thereby allowing the binding of the bHLH proteins to E-box sequences in DNA (39) and driving the expression of muscle-specific genes (46). In general, MyoD and Myf5 are expressed in proliferating myoblasts, whereas myogenin and MRF4 are expressed only after the myoblasts exit the cell cycle (42, 46). The muscle differentiation generally refers to muscle fiber type maturation, and the MyoD protein itself and fiber activity are required for essentially all expression of the 6 kb proximal enhancer/promoter of MyoD in adult fibers (10). MyoD function is regulated in various ways; for example, phosphorylation of MyoD Ser200 (by CDK2) in proliferating myoblasts accelerates its degradation by the ubiquitin pathway (28, 48, 56), CDK4 binding to MyoD in the nucleus inhibits its binding to DNA (75), and acetylation of lysine residues in MyoD by pCAF increases its affinity for DNA, stimulates transcription, and stimulates myogenic conversion of transfected mouse fibroblasts (51).

Here we report that (i) GEP is detectable in skeletal muscle tissue and differentially expressed during the fusion of myoblasts to myotubes; (ii) this differential expression of GEP is mediated by MyoD, a muscle-specific transcription factor; (iii) GEP regulates myogenic differentiation by reducing the levels of transcription factors important for myogenesis, including MyoD; and (iv) GEP regulation of myogenesis is, at least partially, mediated by the transcription factor JunB.

## RESULTS

### GEP is detectable in skeletal muscle, and it exhibits differential expression during the differentiation of C2C12 myoblasts to myotubes

To determine whether GEP is expressed in native skeletal muscle and to establish its subcellular localization, immunostaining for GEP and myosin heavy chain was performed on tibialis anterior muscle of newborn mice. As shown in Figure 1A, GEP is clearly expressed in skeletal muscle and predominantly localized to the myotubes. The expression of GEP in the skeletal muscle tissue of mice suggested that GEP might be involved in muscle differentiation. The mouse myoblast cell line, C2C12, provides a well-established *in vitro* model for muscle differentiation, which is induced by culture with low concentrations of serum (70). The level of endogenous GEP expression during muscle differentiation was determined via real-time PCR and immunofluorescence cell staining. GEP transcript levels were induced early in differentiation, peaked after 3 days of exposure to DM, and returned to near-baseline levels by day 7 (Figure 1B). We then used immunofluorescence cell staining to examine GEP protein levels during the course of myotube formation (Figure 1C). GEP protein levels mirrored GEP mRNA levels with induction during early differentiation. C2C12 cells cultured in GM demonstrated low levels of GEP expression, with positive GEP immunofluorescence that was mainly peri-nuclear (Figure 1C). During differentiation, GEP protein expression increased and GEP became diffusely expressed in the cytoplasm (Figure 1C). These data suggest that GEP expression is coordinately controlled throughout the process of myogenic differentiation.

### MyoD binds to the E–box sequence (CANNTG) in the GEP 5′-flanking region

Having determined that GEP is differentially expressed during myogenic differentiation, we next sought to elucidate the transcriptional control mechanism of the GEP gene. A 1.9-kb segment from the 5′-flanking regulatory region of the human GEP gene (Figure 2A) was found to contain at least five E–box sequences (CANNTG). In addition, these E–box sequences are conserved between human and other mammalian genomes and Figure 2B shows the most proximal E–box sequences of several mammalian genomes available in the GenBank. We then used electrophoretic mobility shift assays (EMSA) to determine whether MyoD can actively bind to these sequences. The MyoD binding sequence (5′-GAGCACCAGCTGCCCTGCT-3′) within the human GEP 5′-flanking region was used as a probe. The EMSA revealed that MyoD does bind to the sequence (Figure 2C, lane 2). This binding was not affected by the addition of unrelated oligonucleotides, but was inhibited by unlabeled probes (Figure 2C, lanes 4 and 5). As expected, the addition of antibodies to MyoD resulted in a “super-shift” of the complex (Figure 2C, lane 3).

We then performed a chromatin immunoprecipitation (ChIP) assay to further confirm that MyoD binds to the E–box sequence in the regulatory region of GEP gene. ChIP was carried out using C2C12 cells transfected with pCMV-MyoD and –1575GEP-luc for 2 days; after reaching confluency, C2C12 cells were shifted to DM for 3 days. DNA-binding proteins were cross-linked to the DNA using formaldehyde. The cells were lysed, the chromatin was sheared by sonication, and protein-DNA complexes were immunoprecipitated using IgG (control) as well as anti-MyoD antibodies. The DNA recovered from the immunoprecipitation was then amplified by PCR using primers that span the MyoD binding site. The PCR results demonstrate that DNA bearing the MyoD binding site was successfully immunoprecipitated by anti-MyoD antibodies (Figure 2D-E, lane 3), but not by control IgG (Figure 2D-E, lane 2). Negative control primers spanning a 5′-regulatory region of GEP gene, approximately 2 kb from the MyoD binding site, did not result in amplification with either the anti-MyoD or control IgG immunoprecipitates (not shown). These results clearly demonstrate that MyoD binds to the E–box sequence within the 5′-

flanking regulatory region of the human GEP gene in a sequence specific manner. In addition, quantitative ChIP analysis revealed that endogenous MyoD and other key transcription factors for myogenesis, including Myf5 and Myogenin, also associated differentially with the regulatory region of the murine GEP gene in the course of myoblast fusion (Figure 2F-H).

### MyoD transactivates GEP-specific reporter genes

We next sought to determine whether the binding of MyoD to E-box sequences results in the induction of GEP expression. For this purpose, four deletion reporter gene plasmids (-1575 GEP-luc, -1087GEP-luc, -978GEP-luc, -271GEP-luc) were generated in which segments containing E-box sequences from the 5'-flanking region of GEP (-1575 to +317, -1087 to +317, -978 to +317, and -271 to +317) were placed upstream of a gene encoding luciferase in the pGL3 vector (Figure 3A). Transfection of the reporter plasmids into C3H10T1/2 fibroblasts resulted in luciferase expression; constructs containing longer lengths of the GEP 5'-flanking region segment demonstrated higher expression levels (Figure 3B). Co-transfection of C3H10T1/2 cells with the reporter plasmids and a MyoD expression plasmid strongly increased reporter gene expression in a dose-dependent manner (Figure 3B). To dissect the importance of the MyoD binding site in the 5'-flanking region of GEP gene, several point mutation reporter constructs of -1575 GEP-luc were generated (Figure 3C) and their transactivation by MyoD tested (Figure 3D). Mutations in the 1<sup>st</sup> MyoD binding site (closer to transcriptional initiation site) and the 2<sup>nd</sup>/3<sup>rd</sup> binding sites resulted in clear reduction in reporter gene activities, whereas mutations in the 4<sup>th</sup> or 5<sup>th</sup> MyoD binding site gave rise to negligible effects on the MyoD-mediated transactivation of the GEP-specific reporter gene.

To further verify the role of MyoD-binding sites in driving GEP expression, the E-box sequence of the -271GEP-luc plasmid was altered (Figure 3E). The alteration of three nucleotides (CTG to TGC) severely reduced the transactivation of the reporter gene by MyoD (Figure 3F). This confirms that the E-box sequences are responsible for driving MyoD-mediated GEP expression.

### MyoD upregulates endogenous GEP expression

To determine whether MyoD upregulates endogenous GEP expression ("in vivo" is deleted), we transfected C3H10T1/2 fibroblasts with MyoD expression plasmid and examined GEP expression with real-time PCR and immunofluorescence microscopy. Transient transfection with pCMV-MyoD led to a 2.7-fold increase in GEP mRNA levels compared with the control (Figure 3G). Analysis using immunofluorescence microscopy indicated that MyoD also induced the expression of GEP protein (Figure 3H). Following fixation and blocking, C3H10T1/2 cultures were stained with anti-GEP and anti-MyoD antibodies. Cells that had taken up the pCMV-MyoD plasmid (as evidenced by increased MyoD expression) also demonstrated increased GEP expression. This demonstrates that MyoD upregulates endogenous GEP expression in the transfected cells. In order to establish whether GEP transcription is regulated by MyoD physiologically, we examined the effect of knockdown of MyoD on GEP mRNA levels in the course of myotube formation of C2C12 cells. The commercial siRNA targeting MyoD significantly suppressed MyoD expression in C2C12 cells (Figure 3I). The knockdown of MyoD dramatically inhibited GEP induction during myoblast fusion (Figure 3J).

### GEP inhibits myotube formation

To determine the role of GEP in muscle differentiation, we first purified recombinant GEP protein (Figure 4A-B). We then utilized phase contrast microscopy to examine the effect of GEP on myogenic differentiation. C2C12 cells were cultured to confluency in GM. Cultures

were then shifted to DM in the presence or absence of 100 ng/ml GEP and incubated for 5 days. Normally, C2C12 cells differentiate into myotubes when cultured in the DM (Figure 4Ca). However, the presence of 100ng/ml GEP prevented a confluent culture of C2C12 myoblasts from forming myotubes in DM (Figure 4Cb). We confirmed these results using fluorescence detection of myosin heavy chain (MHC). MHC-positive cells were reduced dramatically by GEP (Figure 4D).

We also used a GEP expression plasmid to observe the effect of GEP on muscle differentiation in living cells. C2C12 myoblasts were transfected with either pEGFP and pcDNA3.1 (1:20) or pEGFP and pcDNA3.1-GEP (1:20). 24 h following transfection, the cells were switched to the DM for 5 days. C2C12 cells transfected with control pcDNA3.1 formed normal myotubes (Figure 4Ea). However, myotube formation was inhibited in C2C12 cells transfected with pcDNA3.1-GEP (Figure 4Eb). Quantitative analysis shows that GEP reduced the rate of myotube formation by 5-fold when compared with control (Figure 4F).

### Knockdown of GEP stimulates myogenic differentiation

Based on our observation that GEP inhibits myotube formation, we next sought to determine whether the knockdown of GEP via a small-interference RNA approach would enhance myogenesis. The expression of pSUPER-GEP, which encodes GEP-siRNA in the pSUPER vector, efficiently suppressed endogenous GEP expression in C2C12 cells (Figure 5A). C2C12 myoblasts were transfected with either pEGFP and pSUPER (1:20) or pEGFP and pSUPER-GEP (1:20). 24 h following transfection, the cells were switched to DM for 5 days. The C2C12 cells transfected with pSUPER-GEP showed increased rates of myogenic differentiation after 5 days in DM compared with the control (Figure 5B). Quantitative analysis showed that pSUPER-GEP increased the rate of myotube formation compared with the control (Figure 5C). We generated *Grn* (gene encodes GEP protein) knockdown mice and found that the knockdown of *Grn* led to defects in the growth plate chondrocyte differentiation in young mice (19). We then took advantage of these *Grn* knockdown mice to determine whether GEP would have any effect on myogenesis *in vivo*. Interestingly, the muscle fibers of *Grn* knockdown mice were larger in number but noticeably smaller in size when compared with wild-type muscle fibers (Figure 5D-G).

### GEP inhibits the expression of genes specific for myogenesis

Myoblast differentiation is regulated by a host of muscle-specific transcription factors, such as MyoD, Myf5, Myogenin, and MRF4 (17, 42, 45, 46, 64, 65). To investigate the molecular mechanism by which GEP inhibits muscle differentiation, we used real-time PCR and western blotting to detect the expression of MyoD, Myf5, Myogenin, and MHC following GEP exposure. C2C12 cells were cultured to confluency in GM. The cultures were then shifted to DM in the presence or absence of 100 ng/ml GEP for the times indicated. Total RNA was extracted from the cells, and the mRNA levels of MyoD, Myf5, Myogenin, MHC, and GAPDH were measured by real-time PCR. mRNA levels of MyoD, Myogenin, Myf5, and MHC were dramatically reduced following exposure to GEP (Figure 6A). This was confirmed by western blotting with anti-MyoD, anti-MHC, and anti-Tubulin (internal control) antibodies (Figure 6B).

### Inhibition of myogenesis by GEP depends on JunB

To elucidate the pattern of gene expression following stimulation with GEP, we performed microarray analysis. C2C12 cells were treated with GEP for 0, 0.5, 1, 2, and 4 hours, and total mRNA was collected. JunB levels increased as early as 1 hour following GEP stimulation, remained high at 2 hours, and decreased to near-baseline at 4 hours (Figure 7A). To confirm JunB expression profiles under GEP stimulation, confluent C2C12 cells were

shifted to DM and incubated in the presence of 100 ng/ml of recombinant GEP. Cells were harvested at various time points followed by real-time PCR, Western blotting, and immunofluorescent cell staining. As shown in Figure 7B, the level of JunB mRNA increased after GEP addition, reached a peak after 1 hour (4.2 fold), remained unchanged at 2 hours (4.1 fold), and decreased thereafter. We next examined the level of JunB protein by Western blotting (Figure 7C). JunB protein was markedly elevated at 4 hours and remained at high levels thereafter. Immunofluorescent cell staining showed similar results (Figure 7D).

Next, we analyzed whether the inhibition of myogenic differentiation by GEP depends on the induction of JunB expression. We used a p204-specific reporter plasmid, which contains binding sites for MyoD and was well-characterized previously (33, 37). Co-transfection of the reporter plasmid with a MyoD expression plasmid into MyoD-deficient C3H10T1/2 cells strongly increased reporter gene expression (Figure 8B, column 2). The addition of GEP blocked this activation (Figure 8B, column 3). More interestingly, overexpression of JunB had a similar effect in inhibiting the reporter (Figure 8B, column 4), while the silencing of JunB with pSuper-JunB that efficiently suppresses JunB expression (Figure 8A) was able to partially reverse the effect of GEP (Figure 8B column 5).

To further examine the dependence of GEP action on JunB in myogenic differentiation, we measured MHC levels following JunB overexpression and silencing. C2C12 cells were transfected with the JunB expression plasmid, pcDNA3.1-JunB, or the JunB silencing plasmid, pSuper-JunB, as indicated (Figure 8C). The cells were then shifted to DM and cultured with or without GEP. Total RNA was then extracted and MHC expression levels were analyzed. As expected, both GEP and JunB inhibited MHC expression (Figure 8C, columns 2–3). GEP-mediated inhibition was partially lost when JunB was knocked down by siRNA (Figure 8C, column 4) and was restored when JunB was re-expressed (Figure 8C, column 5). These results indicate that the inhibition of myogenic differentiation by GEP depends, at least in part, on JunB.

## DISCUSSION

The discovery that GEP is expressed in muscle tissue is a particularly novel finding that formed the basis of our initial inquiry. Using immunohistochemistry, we found that GEP is clearly expressed in the myotubes of newborn mice (Figure 1A). This stands in contrast to a previous study based on RT-PCR analysis that found low levels of GEP in the muscle tissue of fish (11). Using *in situ* hybridization of adult rodent tissue, another study has also failed to demonstrate GEP expression in differentiated muscle tissue (13). It may be due to the effects of post-transcriptional processing, an immunostaining analysis of GEP at the protein level, that these studies would yield different results than analysis at the mRNA level. However, it is also possible that GEP is differentially expressed at different stages of development and that higher GEP expression levels may predominate in the muscle tissue of newborn mice, in contrast to that of more mature adult rodents.

Our analysis of GEP's role in myogenesis utilized C2C12 myoblasts, which are well-established in the study of muscle differentiation (69, 70). When cultured in low-serum medium, C2C12 myoblasts undergo myogenic differentiation, as evidenced by the spontaneous fusion of C2C12 myoblasts into myotubes. Using this system, we found that GEP was upregulated early in the process of myogenic differentiation, suggesting that the effects of GEP may predominate in the proliferative phase of myogenesis. This is unsurprising given that GEP is a growth factor with pro-proliferative and tumorigenic effects (6). Our data indicate that upregulated GEP levels during myogenesis are mediated by the binding of MyoD to E-box sites within the GEP 5'-flanking region. In our luciferase reporter based assays, we found that one particular E-box sequence is sufficient to stimulate

reporter gene expression (Figure 3). Interestingly, the inclusion of additional binding sites added only modest amounts of reporter activity. Mutation of this site led to the near-complete repression of reporter gene expression, further highlighting the importance of this particular site for MyoD-mediated GEP expression.

GEP is a particularly potent inhibitor of myogenic differentiation. The overexpression of GEP led to significantly decreased myotube formation (Figure 4), while GEP silencing led to an increased number of myotubes *in vitro* and muscle fibers *in vivo* (Figure 5). Furthermore, when C2C12 cells were cultured in DM, the presence of 100 ng/ml GEP not only prevented the expression of myogenic markers, but led to a ~5-fold repression of MyoD and Myf5 (Figure 6A). Our data indicate that GEP inhibits myogenesis through, at least partially, the upregulation of the transcription factor JunB. JunB, which is induced by members of the TGF- $\beta$  superfamily, functions as a key transcriptional factor that drives the cell away from myogenic differentiation and toward osteoblast differentiation (9). Our microarray analysis found that cellular exposure to GEP, in addition to upregulating JunB, also led to higher expression of many other factors that are associated with the TGF- $\beta$  signaling pathway. For example, the exposure of C2C12 cells to GEP led to the increased expression of GADD45B, which is an important mediator of TGF- $\beta$ -induced apoptosis (72). GEP also increased the expression of MADH7 (Smad7), which is induced by TGF- $\beta$ , and acts in a regulatory negative feedback loop to inhibit Smad2/3, which are effectors of TGF- $\beta$  signal transduction (22, 43). Whether GADD45B and Smad7 are also involved in the GEP-mediated inhibition of MyoD remains to be further delineated. Recent studies indicated that GEP acts as the downstream factor of BMP2, a member of TGF- $\beta$  family, in the course of chondrogenesis (19). Similar to GEP, BMP-2 was also reported to inhibit the differentiation of myogenic cells by suppressing the transcriptional factor of MyoD (27, 71). Myostatin, another member of the TGF- $\beta$  superfamily, is also a negative regulator of skeletal muscle growth (18, 29, 40). Loss of myostatin function is associated with an increase in muscle mass (41, 53). Interestingly, the knockdown of GEP led to an increased number of muscle fibers, although they were noticeably smaller in size (Figure 5). The smaller sized myofibers in the *Grn* knockdown mice could be a result of fiber type difference with WT mice, and the knockdown mice may have more fast-type myofibers.

Although the details of the mechanism by which JunB inhibits myogenesis remain unclear, JunB has been shown to block the trans-activation of the muscle creatine kinase (MCK) by myogenin and MyoD (32). MyoD has also been shown to interact directly with the leucine zipper of c-Jun, which is closely related to JunB, both in structure and function (7). Thus, it is possible that the inhibition of myogenesis by JunB occurs through a direct protein-protein interaction among JunB, MyoD, and other transcription factors. Both the upregulation of JunB (Figure 7) and the downregulation of MyoD (Figure 6) were relatively early events in the course of GEP stimulation.

Because of our initial finding that GEP was expressed in murine muscle tissue, it was somewhat surprising to find that GEP inhibits myotube formation (Figure 4–5). This led us to postulate that GEP may belong to a negative feedback loop. Our data indicate that MyoD, GEP, and JunB are participants in a regulatory feedback loop, in which MyoD induces GEP expression, thereby inducing JunB, which in turn inhibits MyoD (Figure 8D). We have also established the specific mechanism by which MyoD induces GEP, namely, by binding to specific sites within the GEP 5'-flanking region. It appears that GEP's action in this regard at least partially depends on JunB, since the silencing of JunB reverses the inhibitory effect of GEP (Figure 8). It is conceivable that intracellular GEP may also exert its inhibitory effect by binding directly to and inhibiting MyoD and/or other transcription factors.

In conclusion, we have identified GEP as a MyoD-inducible growth factor that acts as a novel regulator of myogenic differentiation. GEP is able to inhibit myotube formation *in vitro* and has modulatory effects on muscle tissue development *in vivo*. GEP functions in concert with JunB and MyoD to participate in a regulatory feedback loop, in which the transactivation of GEP expression by MyoD leads to a GEP-mediated suppression of myogenesis, a process that involves the expression of JunB. The elucidation of GEP's role and molecular events involved in myogenic differentiation will better our understanding of normal muscle development and the pathogenesis of muscle disease.

## MATERIALS AND METHODS

### Plasmid constructs

To obtain human GEP protein expression plasmids, full-length GEP cDNA was inserted into the KpnI/ HindIII sites of the pcDNA3.1 expression vector (Clontech). The GEP-specific reporter gene plasmids -1575GEP-luc, -1087GEP-luc, -978GEP-luc, and -271GEP-luc were constructed from four PCR amplicons from human genomic DNA (Clontech) (nucleotides-1575 to +317, -1087 to +317, -978 to +317, and -271 to +317) (Fig. 3A) using four sets of primers (5'-tacgagctcagcaggccagggtgtcttatcc-3' and 5'-gtcaagctctgtgtctccggctgagact-3'; 5'-tacgagctccactggcattgaacatggca-3' and 5'-gtcaagctctgtgtctccggctgagact-3'; 5'-tacgagctccagactcagctcaaggagat-3' and 5'-gtcaagctctgtgtctccggctgagact-3'; 5'-tacgagctcagatcgctccactgcactcc-3' and 5'-gtcaagctctgtgtctccggctgagact-3'). The PCR amplicons were digested with SacI and HindIII and inserted into a pGL3 vector (Promega) previously cleaved with SacI and HindIII. The mutation in the -271GEP-luc plasmid (Figure 3C) was carried out by the Quik Change XL Site-Directed Mutagenesis kit (Stratagene). An oligonucleotide containing three mutations (5'-GGCGACGAGCACCAGTGCCCCTGCTGAGGCTGT-3'; the underlined triplet indicates a C to T, T to G, and G to C change of the original sequence) and a second oligonucleotide (5'-ACAGCCTCAGCAGGGGCACTGGTGCTCGTCCG-3') were used in a PCR reaction under the following conditions: 95 °C for 2 min (1 cycle) and 95 °C for 1 min, 60 °C for 50 s, and 68 °C for 10 min (18 cycles). The presence of the mutations in the plasmid (-271mutantGEP-luc) was confirmed by nucleotide sequencing.

### Generation and selection of GEP and JunB siRNA expression constructs

For GEP silencing, two regions of mouse GEP were targeted by small interfering RNA (siRNA) using the pSUPER vector (OligoEngine) according to the manufacturer's instructions. To generate siRNAs, equimolar amounts of complementary sense and antisense strands were separately mixed, annealed, and slowly cooled to 10 °C in a 50µl reaction buffer (100mM NaCl and 50mM HEPES, pH 7.4). The annealed oligonucleotides were inserted into the BglII/HindIII sites of pSUPER. The resultant plasmids and empty control vector were transfected into C2C12 cells using the Lipofectamine 2000 reagent (Invitrogen), and the GEP expression was determined using real time PCR. The data demonstrated that both siRNAs corresponding to different coding sequences of the GEP gene (5'-GCCTATCCAAGAACTACAC-3' and 5'-AACTACACCACGGATCTCC-3') were able to effectively reduce the expression of mouse GEP. To silence JunB expression, the target sequence 5'-GACCAGGAGCGCATCAAAG-3' has been previously validated (57) and was inserted into the BglII/HindIII sites of the pSUPER vector. The siRNA targeting MyoD and non-targeting siRNA were purchased from Santa Cruz Biotechnology, Inc.

### Generation of GEP-stable cell lines and purification of His-tagged recombinant GEP protein

Stable cell lines were established by transiently transfecting HEK293 cells with pcDNA3.1-GEP plasmid. 24 h following transfection, cells were split into 15-cm culture plates and

selected with 1 mg/ml G418 (Sigma) in Dulbecco's Modified Eagle Medium (DMEM) supplemented with 10% FBS (GIBCO) under an atmosphere of 5% CO<sub>2</sub> at 37°C. After 2 weeks, individual colonies were picked, expanded, and analyzed by Western blotting for GEP expression. Stable cell lines were maintained with G418 (200 µg/ml).

Stable cell lines expressing human Myc/His-GEP were cultured in DMEM supplemented with 10% fetal bovine serum and 200 µg/ml G418. When confluency was reached, the cells were grown with serum-free medium for 2 days. The medium was then collected. ProBond resin (Invitrogen) was prepared by washing with 1 bed volume of binding buffer (0.5 M NaCl and 20 mM sodium phosphate, pH 7.8). The medium and resin were mixed overnight at 4 °C (200 µl of resin/100 ml of medium). The resin was pelleted by centrifugation at 1000 rpm and then washed five times with 10 volumes of binding buffer. Bound protein was eluted by sequential washes with binding buffer containing 250 mM imidazole. The washes and eluted protein fractions were subjected to SDS-PAGE and examined by Coomassie Blue staining and Western blotting to assay the presence and purity of recombinant protein.

### Immunohistochemistry

For histologic examination, tissue samples from newborn mice were immediately fixed in 4% paraformaldehyde/phosphate-buffered saline for 1–3 days at 4°C after dissection. The decalcified specimens were washed 3–4 times for 30 mins (15–20×volumes for all washes) in PBS, dehydrated with gradually increasing concentrations of ethanol (50% ethanol for 1 hour, 70% ethanol for 1 hour, 70% ethanol for 1 hour, 95% ethanol for 1 hour, 95% ethanol for 1 hour, 100% ethanol for 1 hour, 100% ethanol for 1 hour, Xylene for 1 hour, Xylene for 1 hour), and embedded in paraffin. 5 µm formalin fixed paraffin sections of muscle tissue were immunostained for GEP and counterstained with hematoxylin and eosin (HE). The Paraffin sections were rehydrated with graded alcohols to water following procedures (xylene 5 min, xylene 5 min, 100% ethanol 5 min, 100% ethanol 5 min, 95% ethanol 5 min, 95% ethanol 5 min, 70% ethanol 5 min, 70% ethanol 5 min, Distilled H<sub>2</sub>O 1 min) and were pretreated with chondroitinase (Sigma) for 30 min at 37°C followed by protein blocking (Dako Serum-Free Protein Block) for 10 min at room temperature to reduce non-specific staining. The sections were then incubated with anti-GEP antibodies (1:100), which was well-characterized in our previous publications (19, 21, 60, 67). For detection, the sections were incubated with anti-goat antibodies linked to a streptavidin label from the Super Sensitive Alkaline Phosphatase (BioGenex). 0.5 mg/ml DAB (3,3'-diaminobenzidine) in 50mM Tris-Cl substrate (Sigma) was used for visualization, and sections were counterstained with Methyl green. For HE staining, the sections were fixed in 1% glutaraldehyde for 1 min and then immersed in hematoxylin for 30 sec. After washing with alcohol acid and ammonia water, they were immersed in eosin for 15 sec. Following each step, the sections were rinsed with distilled water.

### Luciferase reporter gene assay

C3H10T1/2 cells grown to 70% confluency in DMEM supplemented with 10% FBS in 6-well plates under an atmosphere of 5% CO<sub>2</sub> at 37°C were transfected with 1 µg of one GEP specific reporter plasmid or mutant (–1575 GEP-luc, –1087GEP-luc, –978GEP-luc, –271GEP-luc, –1575GEP(mut1)-luc, –1575GEP(mut2&3)-luc, –1575GEP(mut4)-luc, –1575GEP(mut5)-luc, or –271mutantGEP-luc) using the Lipofectamine 2000 reagent (Invitrogen). Various amounts of pCMV-MyoD were then co-transfected and the pCMV vector was added to bring the total amount of transfected DNA to 5 µg. To detect the effect of JunB on myogenic differentiation, 1 µg p204-specific reporter plasmid was transfected. pCMV-MyoD (2 µg), pcDNA3.1-JunB (1 µg), or psuper-JunB (1 µg) were cotransfected as indicated, and the pCMV vector was added to bring the total amount of transfected DNA to 6 µg. The cells were then cultured with or without GEP. In each case, a pSVgal internal

control plasmid (1 µg) was co-transfected. The cultures were harvested after 48 h following transfection. Cell cultures were rinsed twice with PBS and Add Lysis Solution (100 mM potassium phosphate [pH 7.8], 0.2% Triton X-100, 1 mM DTT) to cover the cells. Cells were detached from the plate with a cell scraper, and the cell lysate was transferred to a microfuge tube. We then froze the cells at  $-80^{\circ}\text{C}$  for 20 minutes, thawed the cells in a  $37^{\circ}\text{C}$  water bath, and vortexed the tube for 10–15 seconds. They were then centrifuged for 2 min to pellet debris. We then transferred extracts (supernatant) to a fresh tube and used them immediately. Luciferase and  $\beta$ -galactosidase activities were analyzed using the Luciferase Reporter Gene Assay (Boehringer Mannheim) and the  $\beta$ -Galactosidase Enzyme Assay System (Promega) by GloMax<sup>®</sup>-96 Microplate Luminometer (Promega) respectively.

### Electrophoretic mobility shift assay (EMSA)

C2C12 cells grown to 70% confluency in GM (DMEM supplemented with 20% FBS) were transfected with pCMV-MyoD. After 48 h, the cells were scraped from the plate by cold PBS, transferred to 10 ml tubes and centrifuged 10 min at 4000 rpm. Cell pellet was resuspended in 400 µl cold buffer (10mM HEPES [pH 7.9], 1 mM DTT, 10 mM KCl, 0.5 mM PMSF, 0.1mM EDTA, 0.1mM EGTA and 1x protease inhibitors [Roche]) by gentle pipetting and placed on ice for 15 mins. We then added 25 µl 10% NP-40, vortexed vigorously for 10 seconds, 14000 rpm centrifuge for 1 min, aspirated the supernatant and kept the pellet. We resuspended the nuclear pellet in a 50ml ice-cold buffer (20mM HEPES [pH 7.9], 1 mM DTT, 0.4 mM NaCl, 1 mM PMSF, 1mM EDTA, 1mM EGTA and 1x protease min, inhibitors [Roche]) and rocked the tube for 30 min at  $4^{\circ}\text{C}$ . It was then centrifuged for 15 min, 14,000 rpm at  $4^{\circ}\text{C}$ . Double-stranded oligonucleotides containing a specific MyoD binding sequence located within the 5'-flanking region of GEP gene (5'-GAGCACCAGCTGCCCTGCT-3') (Oligos synthesized by Integrated DNA Technologies) were labeled with digoxigenin-11-dUTP (Dig) using the reagents provided in the DIG Gel Shift Kit (Roche) according to the manufacturer's instructions. Nuclear extracts (75 ng) were incubated with 310 fmol of labeled probe at room temperature for 15 min in binding reaction solution (20mM HEPES [pH7.6], 0.2% Tween 20, 1mM EDTA, 1mM dithiothreitol, 30mM KCl, 1 mg poly [dI-dC], 0.1 mg poly [L-Lys]). To determine the specificity of binding, the nuclear extracts were incubated with 100-fold molar excess of unlabeled probes, non-relevant oligonucleotides, or 2 µg anti-MyoD antibody (Santa Cruz) for 30 min prior to *in vitro* DNA binding. The protein–DNA complexes were resolved on native pre-run 6% polyacrylamide gels in a  $0.5\times$ TBE buffer at 150 V for 1–1.5 h. The gels were then electrotransferred to positively charged nylon membranes (Roche). The DNA complexes were cross-linked to the membranes at 120 mJ using the Stratilinker UV Crosslinker (Stratagene). Subsequently, electro-blotting and chemiluminescent detection were performed according to the protocol provided in the DIG Gel Shift Kit.

### Chromatin immunoprecipitation (ChIP) assay

C2C12 cells grown to 70% confluency in GM were co-transfected with pCMV-MyoD and  $-1575\text{GEP-luc}$  for 2 days, or C2C12 cells grown to confluency in GM were shifted to DM (DMEM supplemented with 0.5% horse serum) for 3 days. Using a ChIP assay kit (Upstate Biotechnology), cells were treated with formaldehyde (adding formaldehyde directly to culture medium to a final concentration of 1%), incubated at  $37^{\circ}\text{C}$  for 10 minutes, and then washed with cold phosphate buffered saline containing protease inhibitors (1 mM phenylmethylsulfonyl fluoride (PMSF), 1g/mL aprotinin, and 1 g/mL pepstatin A) and lysed in SDS lysis buffer (1% SDS, 10mM EDTA, and 50mM Tris-HCl [pH 8.1]). The lysates were sonicated to shear the DNA to a length between 200 and 500bp. The sonicated supernatant fraction was diluted with ChIP dilution buffer (0.01% SDS, 1% Triton X100, 2mM TrisHCl [pH8.1], and 150mM NaCl) and incubated with anti-MyoD antibodies (Santa Cruz) or preimmune serum with rotation at  $4^{\circ}\text{C}$  overnight. To collect the DNA-protein

complexes, a salmon sperm DNA-protein A-agarose slurry was added to the mixture and incubated with rotation at 4°C for 1 h, and the DNA-protein-agarose was pelleted by centrifugation. After extensive washing of the pellet with a series of buffers (Low Salt Wash Buffer, High Salt Wash Buffer, LiCl Immune Complex Wash Buffer, and 1X TE Buffer [10mM Tris, 8.1, 1 mM EDTA]), the pellet was dissolved in 250 µl elution buffer (1% SDS, 0.1 M NaHCO<sub>3</sub>, 0.01 mg/ml Herring sperm DNA) and centrifuged to remove the agarose. The supernatant fraction was treated with 20 µl of 5M NaCl and heated to 65°C for 4 h to reverse the protein-DNA crosslinking. After treatment with EDTA and proteinase K, the supernatant fraction was extracted with phenol-chloroform and precipitated with ethanol to recover the DNA. For amplification of the GEP 5'-regulatory region, 10% of the immunoprecipitated DNA was amplified using PCR with the primers 5'- CAC AAA TAT TCC CAA TTC A -3' and 5'- TCC TCC CTG CTT CCT C-3' for MyoD binding site in human GEP 5'-regulatory region and 5' - GCA TAA GCA ATG GTC TG - 3' and 5' - GGG TCA GCC ATA CAG TT - 3' for MyoD binding site in mouse GEP 5'-regulatory region. 45 cycles of PCR (at 94°C for 30s, 55°C for 30s, and 72°C for 30s) were performed. The PCR products were analyzed by electrophoresis in a 3% agarose gel.

In order to determine whether endogenous MyoD, Myogenin and Myf5 associate with the regulatory region of GEP gene in the course of myogenesis, C2C12 cells grown to confluency in GM were shifted to DM (DMEM supplemented with 0.5% horse serum) for 1, 3, 5, or 7 days. The cultures were processed as described above and the immunoprecipitated DNAs with anti-MyoD, anti-myogenin, and anti-myf5 antibodies were amplified by quantitative real-time PCR under the following conditions: 40 cycles at 95°C for 15 s and at 60°C for 1 min. GAPDH was employed as an internal control. For each gene, three independent PCRs were performed.

### RNA Preparation and Real Time PCR

C2C12 cells and C3H10T1/2 cells were cultured in GM. After reaching confluency, the C2C12 cultures were shifted to DM in the presence or absence of 100 ng/ml GEP for various times, as indicated. C3H10T1/2 cells at 70% confluency were transfected with pCMV and pCMV-MyoD using Lipofectamine 2000 Reagent (Invitrogen) and cultured for 2 days. C2C12 cells at 70% confluency were co-transfected with pcDNA3.1-JunB and/or pSuper-JunB, as indicated. To determine whether knockdown of MyoD affects the expression of GEP during myotube formation, C2C12 cells were transfected with either control siRNA (CTR) or MyoD siRNA (siMyoD, Santa Cruz Biotechnology) were cultured in GM. After 24 h, the cells were shifted to DM in the presence or absence of 100ng/ml GEP for 5 days. Total RNA was extracted from cells using the RNAeasy Kit (Qiagen). 1 µg total RNA per sample was reverse-transcribed using the ImProm-II Reverse Transcription System (Promega). The following sequence-specific primers were synthesized: 5'- ATGTGGGTCTGATGAGCTG-3' and 5'-GCTCGTTATTCTAGGCCATGTG-3' for mouse GEP, 5'-TGGGATATGGAGCTTCTATCG C-3' and 5'- GGTGAGTCGAAACACGGATCAT-3' for mouse MyoD, 5'- TGAAGGATGGACATGACGGACG-3' and 5'-TTGTGTGCTCCGAAGGCTGCTA-3' for mouse Myf5, 5'-CATCCAGTACATTGAGCGCCTA-3' and 5'- GAGCAAATGATCTCCTGGGTTG-3' for mouse Myogenin, 5'- AGAGCTGACGTGCCTCAATG-3' and 5'-ATGCCTCTTCTTGCCCTTGT-3' for mouse MHC, and 5'-TCACGACGACTTTACGCAG-3' and 5'- CCTTGAGACCCCGATAGGGA-3' for mouse JunB. The following pair of oligonucleotides was used for the internal control: 5'-ATGACATCAAGAAGGTGGTG-3' and 5'-CATACCAGGAAATGAGCTTG-3' for mouse GAPDH. 50-µl SYBR Green PCR reactions were performed in a 96-well optical reaction plate formatted in the 7300 Sequence Detection System (Applied Biosystems) using the following PCR conditions: 40 cycles, 95

°C for 15 s, 60 °C for 1 min. GAPDH was employed as an internal control. The assay was performed in triplicate. The presence of a single specific PCR product was verified by melting curve analysis, confirmed on an agarose gel, and further sequenced by the Applied Biosystems sequencing system (Applied Biosystems).

The comparative  $C_T$  method ( $DDC_T$ ) was used for relative quantitation of gene expression. The calculations for the quantitation start with getting the difference ( $DC_T$ ) between the  $C_T$  values of the target and the normalizer (GAPDH):  $DC_T = C_T(\text{target}) - C_T(\text{normalizer})$ . This value was calculated for each sample to be quantitated. One of these samples, such as day 0, was chosen as the reference (baseline) for each comparison to be made. The absolute  $C_T$  value of GEP mRNA level in RT-PCR was 18–25 cycles. The comparative  $DDC_T$  calculation involves finding the difference between each sample's  $DC_T$  and the baseline's  $DC_T$ . The formula is: comparative expression level =  $2^{-DDC_T}$ . Microsoft Excel was used to do these calculations by simply entering the  $C_T$  values. Finally, the level of reference was set at 1 and the relative expression of gene at other conditions was calculated.

### Microarray analysis

C2C12 cells were cultured in GM. After reaching 90% confluency, the C2C12 cultures were shifted to serum-free DMEM for 24 h. The cells were then stimulated with 100 ng/ml GEP. At various times, total RNA was extracted from the cells for microarray analysis. Transcript expression profiling was assessed at the New York University Genomics Core lab using Affymetrix U133Plus2.0 GeneChips. Briefly, sample processing was performed according to the Affymetrix WT protocol ([www.affymetrix.com/support](http://www.affymetrix.com/support)). The gene-level log-scale robust multiarray analysis sketch algorithm (Affymetrix Expression Console and Partek Genomics Suite 6.2) was used for crude data analysis. Genes were filtered and analyzed using fold change calculations and unsupervised hierarchical cluster analysis (Spotfire DecisionSite for Functional Genomics).

### Immunofluorescent cell staining

Cultures of C2C12 cells and/or C3H10T1/2 cells were plated on glass coverslips, coated with polylysine, and grown in GM. Confluent C2C12 cultures were shifted to DM in the presence or absence of 100 ng/ml GEP. C3H10T1/2 cells at 70% confluency were transfected with pCMV-MyoD using the Lipofectamine 2000 Reagent (Invitrogen) and cultured for 2 days. For staining, the cells were washed with 4°C phosphate buffered saline (PBS), fixed with 100% methanol in the freezer compartment for 5 min, washed twice in 4°C PBS for 5 min, and then incubated with 30% goat serum in phosphate-buffered saline for 30 min. The cells were then incubated with primary antibodies (i.e. goat polyclonal anti-GEP antibodies [Santa Cruz], rabbit polyclonal anti-MyoD antibodies, mouse monoclonal anti-MHC antibodies [Hybridoma Bank], or rabbit polyclonal anti-JunB antibodies [Santa Cruz]) at room temperature for 1 h. After washing with phosphate-buffered saline, the coverslips were incubated with secondary antibody (i.e. chicken anti-goat IgG conjugated with rhodamine [Santa Cruz Biotechnology; diluted 1:100] and goat anti-rabbit IgG conjugated with fluorescein isothiocyanate [Santa Cruz Biotechnology; diluted 1:100]) for 1 h. In each case, the nuclei were stained with 4, 6-diamidino-2-phenylindole (DAPI). The specimens were washed with phosphate-buffered saline and observed under a fluorescence microscope with appropriate optical filters. Microscopic images were captured using Image Pro (Media Cybernetics) and an Olympus microscope. Images were arranged using the Adobe Photoshop program.

### Western blotting

C2C12 cells were cultured in GM. After reaching confluency, the cultures were shifted to DM in the presence or absence of 100 ng/ml GEP for the times indicated. HEK-293EBNA

cells were transfected with pcDNA3.1 vector or pcDNA3.1-JunB for 2 days. Total cell extracts were subjected to SDS-PAGE and examined by Western blotting with rabbit polyclonal MyoD antibody (Santa Cruz), mouse monoclonal anti-MHC antibody (Hybridoma Bank), rabbit polyclonal JunB antibody (Santa Cruz), mouse monoclonal anti-c-myc antibody (Santa Cruz), or mouse monoclonal anti-Tubulin antibody (Promega) (internal control), followed by anti-mouse IgG conjugated to horseradish peroxidase or anti-rabbit IgG conjugated to horseradish peroxidase at 1:1000 dilution. The signals were detected using the ECL chemiluminescent system (Healthcare Life Sciences).

### Statistical analysis

Results were expressed as means  $\pm$  SEMs. Statistical difference was calculated by Student's t-test using SPSS software (SPSS Inc, Chicago, IL).  $P < 0.05$  was considered significant.

### Acknowledgments

This work was funded by NIH research grants AR061484 and AR053210, and a grant from National Psoriasis Foundation (all to C. J. Liu).

### Abbreviations

<b>GEP</b>	granulin-epithelin precursor
<b>PCDGF</b>	P-cell-derived growth factor
<b>FBS</b>	fetal bovine serum
<b>GM</b>	growth medium
<b>DM</b>	differentiation medium
<b>EMSA</b>	Electrophoretic mobility shift assay
<b>ChIP</b>	chromatin immunoprecipitation
<b>PCR</b>	polymerase chain reaction
<b>HRP</b>	horseradish Peroxidase
<b>DAPI</b>	4, 6-diamidino-2-phenylindole
<b>MHC</b>	myosin heavy chain
<b>COMP</b>	cartilage oligomeric matrix protein
<b>TGF-<math>\beta</math></b>	transforming growth factor- $\beta$
<b>TNF<math>\alpha</math></b>	Tumor Necrosis Factor $\alpha$
<b>IL-1<math>\beta</math></b>	interleukin-1 $\beta$
<b>ISH</b>	in situ hybridization
<b>MCK</b>	muscle creatine kinase
<b>HLH</b>	helix-loop-helix

### REFERENCES

1. Anakwe OO, Gerton GL. Acrosome biogenesis begins during meiosis: evidence from the synthesis and distribution of an acrosomal glycoprotein, acrogranin, during guinea pig spermatogenesis. *Biol Reprod.* 1990; 42:317–328. [PubMed: 1692485]

2. Aurade F, Pinset C, Chafey P, Gros F, Montarras D. Myf5, MyoD, myogenin and MRF4 myogenic derivatives of the embryonic mesenchymal cell line C3H10T1/2 exhibit the same adult muscle phenotype. *Differentiation*. 1994; 55:185–192. [PubMed: 8187980]
3. Baba T, Hoff HB 3rd, Nemoto H, Lee H, Orth J, Arai Y, Gerton GL. Acrogranin, an acrosomal cysteine-rich glycoprotein, is the precursor of the growth-modulating peptides, granulins, and epithelins, and is expressed in somatic as well as male germ cells. *Mol Reprod Dev*. 1993; 34:233–243. [PubMed: 8471244]
4. Barreda DR, Hanington PC, Walsh CK, Wong P, Belosevic M. Differentially expressed genes that encode potential markers of goldfish macrophage development in vitro. *Dev Comp Immunol*. 2004; 28:727–746. [PubMed: 15043942]
5. Bateman A, Belcourt D, Bennett H, Lazure C, Solomon S. Granulins, a novel class of peptide from leukocytes. *Biochem Biophys Res Commun*. 1990; 173:1161–1168. [PubMed: 2268320]
6. Bateman A, Bennett HP. The granulin gene family: from cancer to dementia. *Bioessays*. 2009; 31:1245–1254. [PubMed: 19795409]
7. Bengal E, Ransone L, Scharfmann R, Dwarki VJ, Tapscott SJ, Weintraub H, Verma IM. Functional antagonism between c-Jun and MyoD proteins: a direct physical association. *Cell*. 1992; 68:507–519. [PubMed: 1310896]
8. Braun T, Buschhausen-Denker G, Bober E, Tannich E, Arnold HH. A novel human muscle factor related to but distinct from MyoD1 induces myogenic conversion in 10T1/2 fibroblasts. *Embo J*. 1989; 8:701–709. [PubMed: 2721498]
9. Chaux E, Lopez-Rovira T, Rosa JL, Bartrons R, Ventura F. Jun B is involved in the inhibition of myogenic differentiation by bone morphogenetic protein-2. *J Biol Chem*. 1998; 273:537–543. [PubMed: 9417113]
10. Charge SB, Brack AS, Bayol SA, Hughes SM. MyoD- and nerve-dependent maintenance of MyoD expression in mature muscle fibres acts through the DRR/PRR element. *BMC Dev Biol*. 2008; 8:5. [PubMed: 18215268]
11. Chen X, Baumel M, Mannel DN, Howard OM, Oppenheim JJ. Interaction of TNF with TNF receptor type 2 promotes expansion and function of mouse CD4+CD25+ T regulatory cells. *J Immunol*. 2007; 179:154–161. [PubMed: 17579033]
12. Choi J, Costa ML, Mermelstein CS, Chagas C, Holtzer S, Holtzer H. MyoD converts primary dermal fibroblasts, chondroblasts, smooth muscle, and retinal pigmented epithelial cells into striated mononucleated myoblasts and multinucleated myotubes. *Proc Natl Acad Sci U S A*. 1990; 87:7988–7992. [PubMed: 2172969]
13. Daniel R, He Z, Carmichael KP, Halper J, Bateman A. Cellular localization of gene expression for progranulin. *J Histochem Cytochem*. 2000; 48:999–1009. [PubMed: 10858277]
14. Davidson B, Alejandro E, Florenes VA, Goderstad JM, Risberg B, Kristensen GB, Trope CG, Kohn EC. Granulin-epithelin precursor is a novel prognostic marker in epithelial ovarian carcinoma. *Cancer*. 2004; 100:2139–2147. [PubMed: 15139056]
15. Davis RL, Weintraub H, Lassar AB. Expression of a single transfected cDNA converts fibroblasts to myoblasts. *Cell*. 1987; 51:987–1000. [PubMed: 3690668]
16. Edmondson DG, Olson EN. A gene with homology to the myc similarity region of MyoD1 is expressed during myogenesis and is sufficient to activate the muscle differentiation program. *Genes Dev*. 1989; 3:628–640. [PubMed: 2473006]
17. Edmondson DG, Olson EN. Helix-loop-helix proteins as regulators of muscle-specific transcription. *J Biol Chem*. 1993; 268:755–758. [PubMed: 8380414]
18. Elkasrawy MN, Hamrick MW. Myostatin (GDF-8) as a key factor linking muscle mass and bone structure. *J Musculoskelet Neuronal Interact*. 2010; 10:56–63. [PubMed: 20190380]
19. Feng JQ, Guo FJ, Jiang BC, Zhang Y, Frenkel S, Wang DW, Tang W, Xie Y, Liu CJ. Granulin epithelin precursor: a bone morphogenetic protein 2-inducible growth factor that activates Erk1/2 signaling and JunB transcription factor in chondrogenesis. *FASEB J*. 2010; 24:1879–1892. [PubMed: 20124436]
20. Gonzalez EM, Mongiat M, Slater SJ, Baffa R, Izzo RV. A novel interaction between perlecan protein core and progranulin: potential effects on tumor growth. *J Biol Chem*. 2003; 278:38113–38116. [PubMed: 12900424]

21. Guo F, Lai Y, Tian Q, Lin EA, Kong L, Liu C. Granulin-epithelin precursor binds directly to ADAMTS-7 and ADAMTS-12 and inhibits their degradation of cartilage oligomeric matrix protein. *Arthritis Rheum.* 2010; 62:2023–2036. [PubMed: 20506400]
22. Hayashi H, Abdollah S, Qiu Y, Cai J, Xu YY, Grinnell BW, Richardson MA, Topper JN, Gimbrone MA Jr, Wrana JL, Falb D. The MAD-related protein Smad7 associates with the TGFbeta receptor and functions as an antagonist of TGFbeta signaling. *Cell.* 1997; 89:1165–1173. [PubMed: 9215638]
23. He Z, Bateman A. Progranulin (granulin-epithelin precursor, PC-cell-derived growth factor, acrogranin) mediates tissue repair and tumorigenesis. *J Mol Med.* 2003; 81:600–612. [PubMed: 12928786]
24. He Z, Ong CH, Halper J, Bateman A. Progranulin is a mediator of the wound response. *Nat Med.* 2003; 9:225–229. [PubMed: 12524533]
25. Jones MB, Spooner M, Kohn EC. The granulin-epithelin precursor: a putative new growth factor for ovarian cancer. *Gynecol Oncol.* 2003; 88:S136–S139. [PubMed: 12586105]
26. Justen HP, Grunewald E, Totzke G, Gouni-Berthold I, Sachinidis A, Wessinghage D, Vetter H, Schulze-Osthoff K, Ko Y. Differential gene expression in synovium of rheumatoid arthritis and osteoarthritis. *Mol Cell Biol Res Commun.* 2000; 3:165–172. [PubMed: 10860865]
27. Katagiri T, Akiyama S, Namiki M, Komaki M, Yamaguchi A, Rosen V, Wozney JM, Fujisawa-Sehara A, Suda T. Bone morphogenetic protein-2 inhibits terminal differentiation of myogenic cells by suppressing the transcriptional activity of MyoD and myogenin. *Exp Cell Res.* 1997; 230:342–351. [PubMed: 9024793]
28. Kitzmann M, Vandromme M, Schaeffer V, Carnac G, Labbe JC, Lamb N, Fernandez A. cdk1- and cdk2-mediated phosphorylation of MyoD Ser200 in growing C2 myoblasts: role in modulating MyoD half-life and myogenic activity. *Mol Cell Biol.* 1999; 19:3167–3176. [PubMed: 10082583]
29. Kollias HD, McDermott JC. Transforming growth factor-beta and myostatin signaling in skeletal muscle. *J Appl Physiol.* 2008; 104:579–587. [PubMed: 18032576]
30. Lassar AB, Davis RL, Wright WE, Kadesch T, Murre C, Voronova A, Baltimore D, Weintraub H. Functional activity of myogenic HLH proteins requires hetero-oligomerization with E12/E47-like proteins in vivo. *Cell.* 1991; 66:305–315. [PubMed: 1649701]
31. Lassar AB, Skapek SX, Novitch B. Regulatory mechanisms that coordinate skeletal muscle differentiation and cell cycle withdrawal. *Curr Opin Cell Biol.* 1994; 6:788–794. [PubMed: 7880524]
32. Li L, Zhou J, James G, Heller-Harrison R, Czech MP, Olson EN. FGF inactivates myogenic helix-loop-helix proteins through phosphorylation of a conserved protein kinase C site in their DNA-binding domains. *Cell.* 1992; 71:1181–1194. [PubMed: 1335366]
33. Liu C, Wang H, Zhao Z, Yu S, Lu YB, Meyer J, Chatterjee G, Deschamps S, Roe BA, Lengyel P. MyoD-dependent induction during myoblast differentiation of p204, a protein also inducible by interferon. *Mol Cell Biol.* 2000; 20:7024–7036. [PubMed: 10958697]
34. Liu CJ. ADAMTS-7 and ADAMTS-12 in arthritis. *Nature Clinical Practice Rheumatology.* 2008
35. Liu CJ. Progranulin: A promising therapeutic target for rheumatoid arthritis. *FEBS Lett.* 2011
36. Liu CJ, Bosch X. Progranulin: A growth factor, a novel TNFR ligand and a drug target. *Pharmacol Ther.* 2011
37. Liu CJ, Ding B, Wang H, Lengyel P. The MyoD-inducible p204 protein overcomes the inhibition of myoblast differentiation by Id proteins. *Mol Cell Biol.* 2002; 22:2893–2905. [PubMed: 11940648]
38. Lu R, Serrero G. Inhibition of PC cell-derived growth factor (PCDGF, epithelin/granulin precursor) expression by antisense PCDGF cDNA transfection inhibits tumorigenicity of the human breast carcinoma cell line MDA-MB-468. *Proc Natl Acad Sci U S A.* 2000; 97:3993–3998. [PubMed: 10760271]
39. Massari ME, Murre C. Helix-loop-helix proteins: regulators of transcription in eucaryotic organisms. *Mol Cell Biol.* 2000; 20:429–440. [PubMed: 10611221]
40. McPherron AC, Lawler AM, Lee SJ. Regulation of skeletal muscle mass in mice by a new TGF-beta superfamily member. *Nature.* 1997; 387:83–90. [PubMed: 9139826]

41. McPherron AC, Lee SJ. Suppression of body fat accumulation in myostatin-deficient mice. *J Clin Invest.* 2002; 109:595–601. [PubMed: 11877467]
42. Megeney LA, Rudnicki MA. Determination versus differentiation and the MyoD family of transcription factors. *Biochem Cell Biol.* 1995; 73:723–732. [PubMed: 8714693]
43. Nakao A, Afrakhte M, Moren A, Nakayama T, Christian JL, Heuchel R, Itoh S, Kawabata M, Heldin NE, Heldin CH, ten Dijke P. Identification of Smad7, a TGFbeta-inducible antagonist of TGF-beta signalling. *Nature.* 1997; 389:631–635. [PubMed: 9335507]
44. Olson EN. Interplay between proliferation and differentiation within the myogenic lineage. *Dev Biol.* 1992; 154:261–272. [PubMed: 1330787]
45. Olson EN. MyoD family: a paradigm for development? *Genes Dev.* 1990; 4:1454–1461. [PubMed: 2253873]
46. Olson EN, Klein WH. bHLH factors in muscle development: dead lines and commitments, what to leave in and what to leave out. *Genes Dev.* 1994; 8:1–8. [PubMed: 8288123]
47. Plowman GD, Green JM, Neubauer MG, Buckley SD, McDonald VL, Todaro GJ, Shoyab M. The epithelin precursor encodes two proteins with opposing activities on epithelial cell growth. *J Biol Chem.* 1992; 267:13073–13078. [PubMed: 1618805]
48. Reynaud EG, Pospel K, Guillier M, Leibovitch MP, Leibovitch SA. p57(Kip2) stabilizes the MyoD protein by inhibiting cyclin E-Cdk2 kinase activity in growing myoblasts. *Mol Cell Biol.* 1999; 19:7621–7629. [PubMed: 10523650]
49. Rhodes SJ, Konieczny SF. Identification of MRF4: a new member of the muscle regulatory factor gene family. *Genes Dev.* 1989; 3:2050–2061. [PubMed: 2560751]
50. Rudnicki MA, Jaenisch R. The MyoD family of transcription factors and skeletal myogenesis. *Bioessays.* 1995; 17:203–209. [PubMed: 7748174]
51. Sartorelli V, Puri PL, Hamamori Y, Ogryzko V, Chung G, Nakatani Y, Wang JY, Kedes L. Acetylation of MyoD directed by PCAF is necessary for the execution of the muscle program. *Mol Cell.* 1999; 4:725–734. [PubMed: 10619020]
52. Schafer BW, Blakely BT, Darlington GJ, Blau HM. Effect of cell history on response to helix-loop-helix family of myogenic regulators. *Nature.* 1990; 344:454–458. [PubMed: 2157160]
53. Schuelke M, Wagner KR, Stolz LE, Hubner C, Riebel T, Komen W, Braun T, Tobin JF, Lee SJ. Myostatin mutation associated with gross muscle hypertrophy in a child. *N Engl J Med.* 2004; 350:2682–2688. [PubMed: 15215484]
54. Sell C, Dumenil G, Deveaud C, Miura M, Coppola D, DeAngelis T, Rubin R, Efstratiadis A, Baserga R. Effect of a null mutation of the insulin-like growth factor I receptor gene on growth and transformation of mouse embryo fibroblasts. *Mol Cell Biol.* 1994; 14:3604–3612. [PubMed: 8196606]
55. Shoyab M, McDonald VL, Byles C, Todaro GJ, Plowman GD. Epithelins 1 and 2: isolation and characterization of two cysteine-rich growth-modulating proteins. *Proc Natl Acad Sci U S A.* 1990; 87:7912–7916. [PubMed: 2236009]
56. Song A, Wang Q, Goebel MG, Harrington MA. Phosphorylation of nuclear MyoD is required for its rapid degradation. *Mol Cell Biol.* 1998; 18:4994–4999. [PubMed: 9710583]
57. Sreeramani R, Chaudhry A, McMahon M, Sherr CJ, Inoue K. Ras-Raf-Arf signaling critically depends on the Dmp1 transcription factor. *Mol Cell Biol.* 2005; 25:220–232. [PubMed: 15601844]
58. Sun X, Gulyas M, Hjerpe A. Mesothelial differentiation as reflected by differential gene expression. *Am J Respir Cell Mol Biol.* 2004; 30:510–518. [PubMed: 14551161]
59. Suzuki M, Nishihara M. Granulin precursor gene: a sex steroid-inducible gene involved in sexual differentiation of the rat brain. *Mol Genet Metab.* 2002; 75:31–37. [PubMed: 11825061]
60. Tang W, Lu Y, Tian QY, Zhang Y, Guo FJ, Liu GY, Syed NM, Lai Y, Lin EA, Kong L, Su J, Yin F, Ding AH, Zanin-Zhorov A, Dustin ML, Tao J, Craft J, Yin Z, Feng JQ, Abramson SB, Yu XP, Liu CJ. The Growth Factor Progranulin Binds to TNF Receptors and Is Therapeutic Against Inflammatory Arthritis in Mice. *Science.* 2011; 332:478–484. [PubMed: 21393509]
61. Tang W, Lu Y, Tian QY, Zhang Y, Guo FJ, Liu GY, Syed NM, Lai Y, Lin EA, Kong L, Su J, Yin F, Ding AH, Zanin-Zhorov A, Dustin ML, Tao J, Craft J, Yin Z, Feng JQ, Abramson SB, Yu XP, Liu CJ. The growth factor progranulin binds to TNF receptors and is therapeutic against inflammatory arthritis in mice. *Science.* 2011; 332:478–484. [PubMed: 21393509]

62. Thayer MJ, Tapscott SJ, Davis RL, Wright WE, Lassar AB, Weintraub H. Positive autoregulation of the myogenic determination gene MyoD1. *Cell*. 1989; 58:241–248. [PubMed: 2546677]
63. Wang W, Hayashi J, Kim WE, Serrero G. PC cell-derived growth factor (granulin precursor) expression and action in human multiple myeloma. *Clin Cancer Res*. 2003; 9:2221–2228. [PubMed: 12796389]
64. Weintraub H, Davis R, Tapscott S, Thayer M, Krause M, Benezra R, Blackwell TK, Turner D, Rupp R, Hollenberg S, et al. The myoD gene family: nodal point during specification of the muscle cell lineage. *Science*. 1991; 251:761–766. [PubMed: 1846704]
65. Wright WE. Muscle basic helix-loop-helix proteins and the regulation of myogenesis. *Curr Opin Genet Dev*. 1992; 2:243–248. [PubMed: 1638118]
66. Wright WE, Sassoon DA, Lin VK. Myogenin, a factor regulating myogenesis, has a domain homologous to MyoD. *Cell*. 1989; 56:607–617. [PubMed: 2537150]
67. Xu K, Zhang Y, Ilalov K, Carlson CS, Feng JQ, Di Cesare PE, Liu CJ. Cartilage oligomeric matrix protein associates with granulin-epithelin precursor (GEP) and potentiates GEP-stimulated chondrocyte proliferation. *J Biol Chem*. 2007; 282:11347–11355. [PubMed: 17307734]
68. Xu SQ, Tang D, Chamberlain S, Pronk G, Masiarz FR, Kaur S, Prisco M, Zanocco-Marani T, Baserga R. The granulin/epithelin precursor abrogates the requirement for the insulin-like growth factor 1 receptor for growth in vitro. *J Biol Chem*. 1998; 273:20078–20083. [PubMed: 9685348]
69. Yaffe D. Retention of differentiation potentialities during prolonged cultivation of myogenic cells. *Proc Natl Acad Sci U S A*. 1968; 61:477–483. [PubMed: 5245982]
70. Yaffe D, Saxel O. Serial passaging and differentiation of myogenic cells isolated from dystrophic mouse muscle. *Nature*. 1977; 270:725–727. [PubMed: 563524]
71. Yamamoto N, Akiyama S, Katagiri T, Namiki M, Kurokawa T, Suda T. Smad1 and smad5 act downstream of intracellular signalings of BMP-2 that inhibits myogenic differentiation and induces osteoblast differentiation in C2C12 myoblasts. *Biochem Biophys Res Commun*. 1997; 238:574–580. [PubMed: 9299554]
72. Yoo J, Ghiassi M, Jirmanova L, Balliet AG, Hoffman B, Fornace AJ Jr, Liebermann DA, Bottinger EP, Roberts AB. Transforming growth factor-beta-induced apoptosis is mediated by Smad-dependent expression of GADD45b through p38 activation. *J Biol Chem*. 2003; 278:43001–43007. [PubMed: 12933797]
73. Zanocco-Marani T, Bateman A, Romano G, Valentini B, He ZH, Baserga R. Biological activities and signaling pathways of the granulin/epithelin precursor. *Cancer Res*. 1999; 59:5331–5340. [PubMed: 10537317]
74. Zhang H, Serrero G. Inhibition of tumorigenicity of the teratoma PC cell line by transfection with antisense cDNA for PC cell-derived growth factor (PCDGF, epithelin/granulin precursor). *Proc Natl Acad Sci U S A*. 1998; 95:14202–14207. [PubMed: 9826678]
75. Zhang JM, Zhao X, Wei Q, Paterson BM. Direct inhibition of G(1) cdk kinase activity by MyoD promotes myoblast cell cycle withdrawal and terminal differentiation. *Embo J*. 1999; 18:6983–6993. [PubMed: 10601020]
76. Zhou J, Gao G, Crabb JW, Serrero G. Purification of an autocrine growth factor homologous with mouse epithelin precursor from a highly tumorigenic cell line. *J Biol Chem*. 1993; 268:10863–10869. [PubMed: 8496151]
77. Zhu J, Nathan C, Jin W, Sim D, Ashcroft GS, Wahl SM, Lacomis L, Erdjument-Bromage H, Tempst P, Wright CD, Ding A. Conversion of proepithelin to epithelins: roles of SLPI and elastase in host defense and wound repair. *Cell*. 2002; 111:867–878. [PubMed: 12526812]

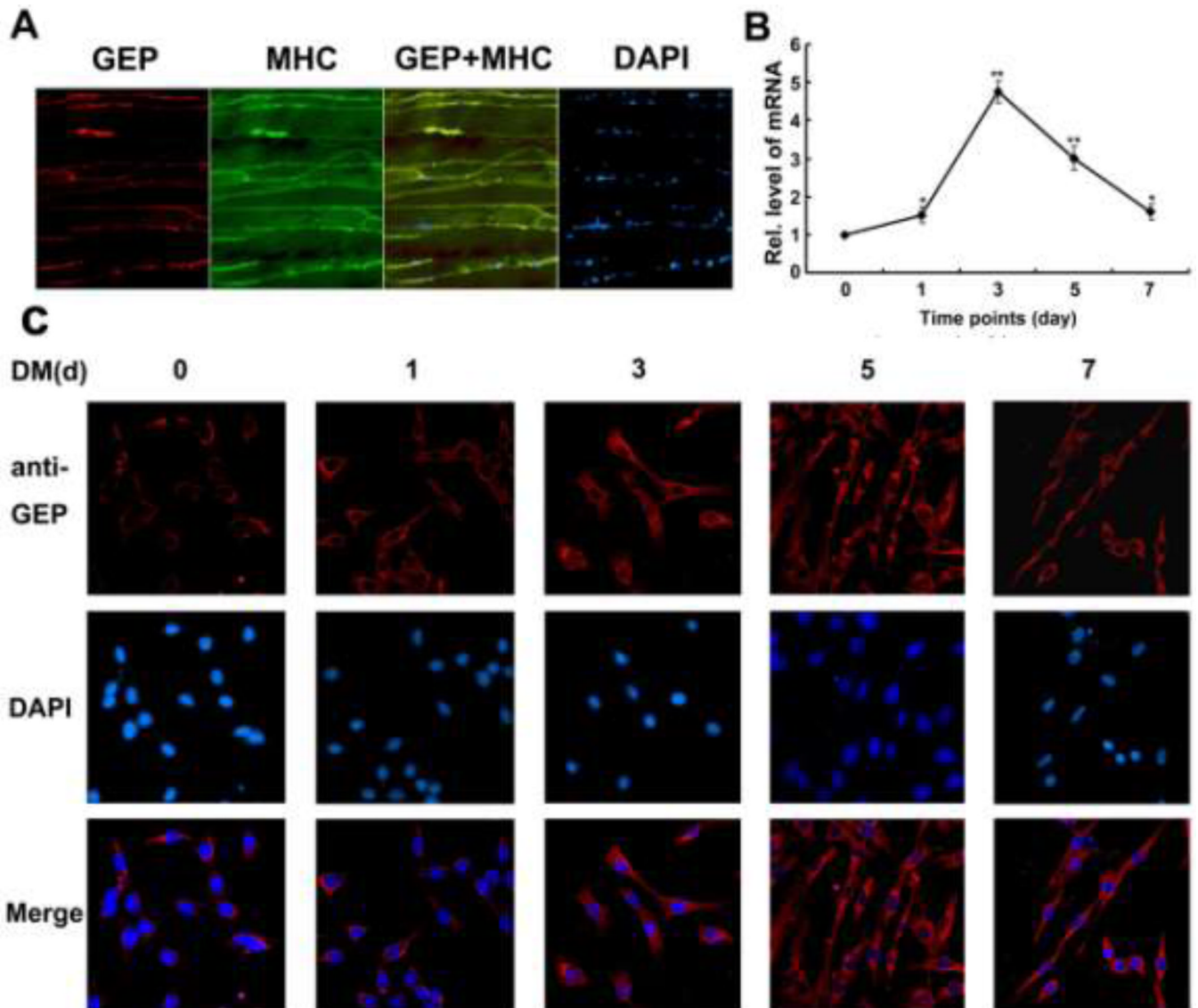


**FIGURE 1. Expression of GEP throughout the course of myotube formation**

**Panel A. GEP is expressed in newborn mouse myocytes.** Newborn mouse muscle tissue dissected, sectioned, and immunostained with anti-GEP antibody (red), and anti-myosin heavy chain (MHC) monoclonal antibody (green). The nuclei were stained with DAPI (blue). **Panel B. GEP is differentially expressed during C2C12 myoblast fusion.** C2C12 cells were cultured in GM. After reaching confluency, the C2C12 cultures were exposed to DM (day 0). At various time points, total RNA was extracted from the cells and the mRNA levels of GEP and GAPDH were measured by real-time PCR. GEP expression was normalized against GAPDH endogenous control. The units are arbitrary, and the relative level of GEP mRNA on day 0 was set to 1. Experiments were repeated three times. Compared to the day 0 time point \*,  $P < 0.05$ ; \*\*,  $P < 0.01$ . **Panel C. GEP Immunofluorescence cell staining.** C2C12 cells were cultured in the presence of GM and switched to DM on day 0. At various time points, the cells were washed, fixed with methanol, and incubated with anti-GEP antibodies. Fluorescence from a secondary rhodamine-conjugated antibody was then detected (red). The nuclei were stained with DAPI (blue).

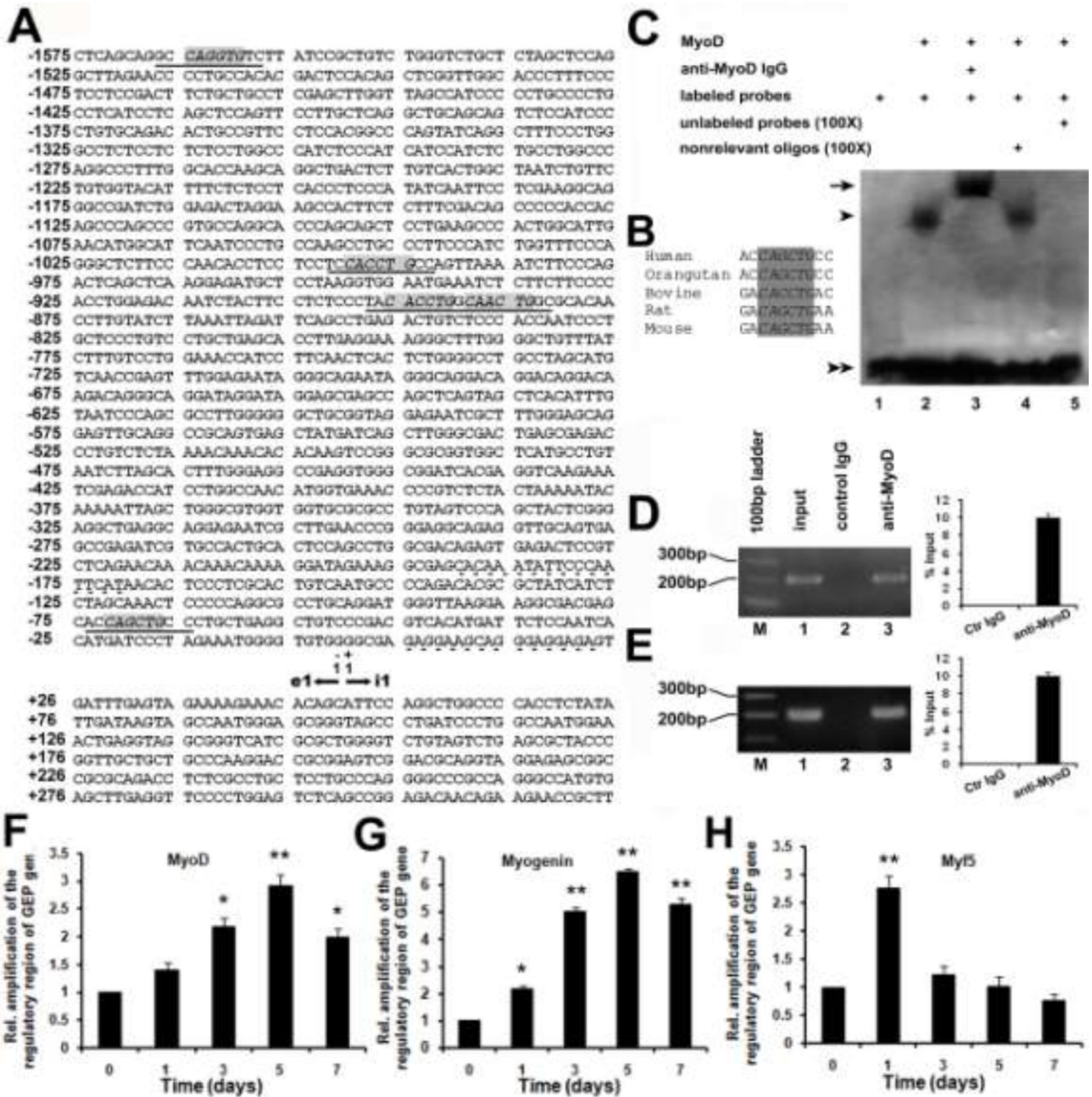


**FIGURE 2. MyoD binds to E-box (CANNTG) sequences in the 5'-flanking regulatory region of GEP gene**

**Panel A.** Nucleotide sequence of a ~1.9-Kb segment from the 5'-flanking region of human GEP gene. MyoD-responsive elements are underlined, and their core sequences (E-box sequence CANNTG) are highlighted. The border between exon 1 and intron 1 is indicated by "e1←→i1." As indicated, the last nucleotide of exon 1 is designated as nucleotide -1, and first nucleotide of intron 1 is designated as nucleotide +1. The numerical designation of the first nucleotide in each row is indicated by the numbers on the left. **Panel B.** Comparison of the most proximal E-box between human and other mammalian genomes. E-box sequence CANNTG is highlighted. **Panel C.** Electrophoresis Mobility

**Shift Assay.** Nuclear extracts were prepared from C2C12 cells transfected with pCMV-MyoD and incubated with a Dig-labeled segment from the 5'-flanking region of GEP (-1025 to -826) (see Fig. 2A) for 30 min at room temperature. The MyoD-DNA complexes were resolved on a 6% non-denaturing polyacrylamide gel. For competition experiments, a 100-fold excess of the unlabeled probes or unrelated oligonucleotides were added to the reaction mixture at time zero. Where indicated, anti-MyoD IgG (0.5 $\mu$ g) was added to the reaction mixture after a 20-min incubation, and the incubation was continued for a further 15 min prior to gel electrophoresis. The MyoD-DNA complex (arrow head), the MyoD-DNA complex supershifted by anti-MyoD IgG (arrow), and the unbound probes (double arrowheads) are indicated. **Panel D-E. Interaction between transfected MyoD and GEP 5'-flanking region, assayed by ChIP.** C2C12 cells were cotransfected with pCMV-MyoD and -1575GEP-luc in GM (Panel C), or shifted to DM (Panel D). Following crosslinking with formaldehyde, cell lysates were prepared, sonicated, and subjected to immunoprecipitation with anti-MyoD and control IgG. Purified DNA from the cell lysate as input DNA and DNA recovered from immunoprecipitation were amplified by PCR using specific primers (primer locations indicated by dotted line in Fig. 2A, PCR product size: 211bp) for the MyoD binding site within the human GEP 5'-flanking region. **Panel F-H. Interaction between endogenous MyoD and GEP 5'-flanking region, assayed by quantitative ChIP.** C2C12 cells were shifted to DM and incubated for various time points, as indicated. The cultures were processed as described above and cell lysates were immunoprecipitated with anti-MyoD (Panel E), anti-myogenin (Panel F), anti-Myf5 (Panel G) and control IgG. Recovered DNAs from immunoprecipitation were amplified by quantitative PCR (The target for mouse GEP 5'-flanking region specific primers was between -932 and -732 upstream the mouse GEP gene, PCR product size: 201bp), the amplification level of the target gene was normalized to the Input, and the relative level on day 0 was set to 1. All experiments were repeated three times. Error bars indicate SEM. \*,  $P < 0.05$ ; \*\*,  $P < 0.01$ .

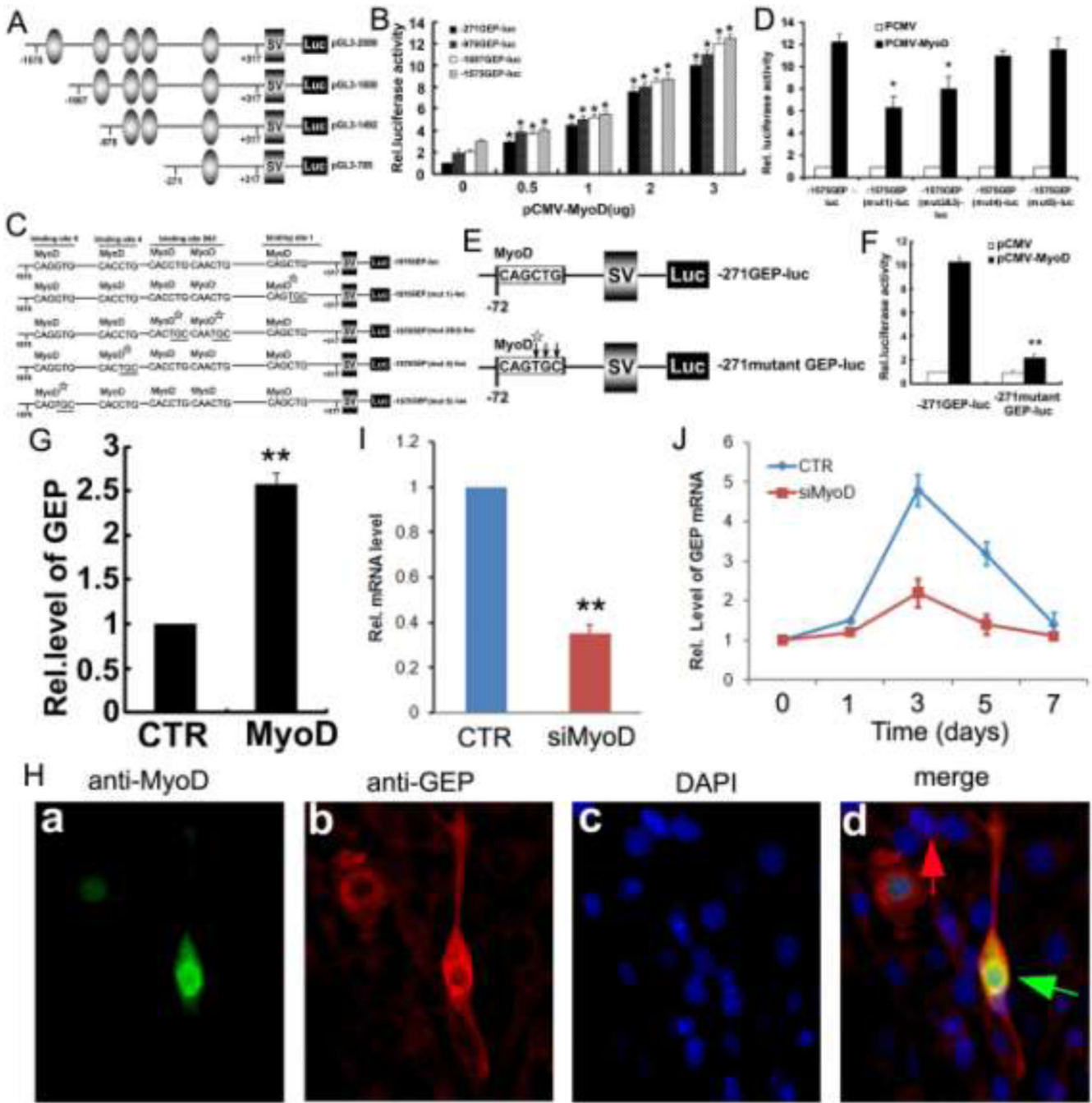


**FIGURE 3. MyoD transactivates GEP-specific reporter genes and upregulates the expression of GEP**

**Panel A. Schematic representation of four GEP-specific reporter gene constructs.** The indicated segments from the 5'-flanking region of the GEP gene were linked to a simian virus 40 5'-flanking region (SV) and a DNA segment encoding luciferase (Luc). E-box sequences are indicated by ovals. The numbers indicate the distance, in nucleotides, from the first nucleotide of intron 1. **Panel B. MyoD can drive the expression of GEP-specific reporter gene in C3H10T1/2 cells.** The indicated reporter constructs were transfected into C3H10T1/2 cells together with various amounts of a pCMV-MyoD expression plasmid, as indicated, along with a pSVgal internal control plasmid. 48 h following transfection, the

cultures were harvested and lysed, and  $\beta$ -galactosidase and luciferase activities were determined. Luciferase activity was normalized to  $\beta$ -galactosidase activity. The relative luciferase activity of the leftmost bar was set to 1. Compared to the cells untransfected with pCMV-MyoD plasmid (0) in each group of indicated reporter constructs \*,  $P < 0.05$ . **Panel C. Schematic of four mutants of -1575 GEP-luc reporter gene.** The E-box sequence in the -1575 GEP-luc reporter construct was altered, as indicated. The mutant MyoD binding sites are indicated by stars; mutant nucleotides are indicated by underline. **Panel D. Mutations of the MyoD-binding sites results in the reduction in Myo-D-activated reporter gene expression.** The indicated reporter construct and the pSVgal internal control plasmid were transfected into C3H10T1/2 cells together with 3 mg of pCMV (control) or the pCMV-MyoD expression plasmid. The cultures were processed and the reporter gene activities analyzed as described in B. Compared to wildtype reporter construct \*,  $P < 0.05$ . **Panel E. Schematic of mutated MyoD binding site in -271GEP-luc reporter construct.** The MyoD-binding site in the -271GEP-luc reporter construct was altered, as indicated. The mutant MyoD binding site is indicated by a star; mutant nucleotides are indicated by arrows. Compared to wildtype reporter construct \*\*,  $P < 0.01$ . **Panel F. Alteration of the MyoD-binding site abolishes Myo-D-induced reporter gene expression.** C3H10T1/2 cells were transfected, processed, and the reporter gene activities analyzed as described in B. **Panel G. MyoD upregulates endogenous GEP mRNA expression.** C3H10T1/2 cells at 70% confluency were transfected with pCMV or pCMV-MyoD and cultured for 2 days. Total RNA was extracted from cells and the mRNA levels of GEP and GAPDH were measured by real-time PCR. The units are arbitrary, the relative GEP mRNA level of pCMV transfection group (CTR) was set to 1. \*\*,  $P < 0.01$ . **Panel H. Immunofluorescence staining of MyoD-upregulated GEP expression.** C3H10T1/2 cells at 70% confluency were transfected with pCMV-MyoD and cultured for 2 days. Following fixation and blocking, the cultures were stained with anti-GEP (green) and anti-MyoD antibodies (red). The nuclei were stained with 4, 6-diamidino-2-phenylindole (DAPI) (blue). The representative cells transfected and untransfected with the MyoD-expressing plasmid are indicated with green and red arrows, respectively. **Panel I & J. Silencing of MyoD inhibits GEP expression in the course of myogenesis.** In panel I, C2C12 cells were transfected with either control siRNA (CTR) or MyoD siRNA (siMyoD, Santa Cruz Biotechnology) and total RNA was collected for real-time RT-PCR. Expression of MyoD was normalized against the GAPDH endogenous control. The normalized values were then calibrated against the control value, here set to 1. \*\*,  $P < 0.01$ . In panel J, C2C12 cells transfected with either control siRNA (CTR) or MyoD siRNA (siMyoD) were cultured in GM. After reaching confluency, the cultures were shifted to DM (day 0). At various time points, total RNA was extracted from the cells and the mRNA levels of GEP and GAPDH were measured by real-time PCR. The units are arbitrary, and the relative level of GEP mRNA on day 0 was set to 1. All experiments were repeated three times. Bar graphs show mean  $\pm$  SEM.

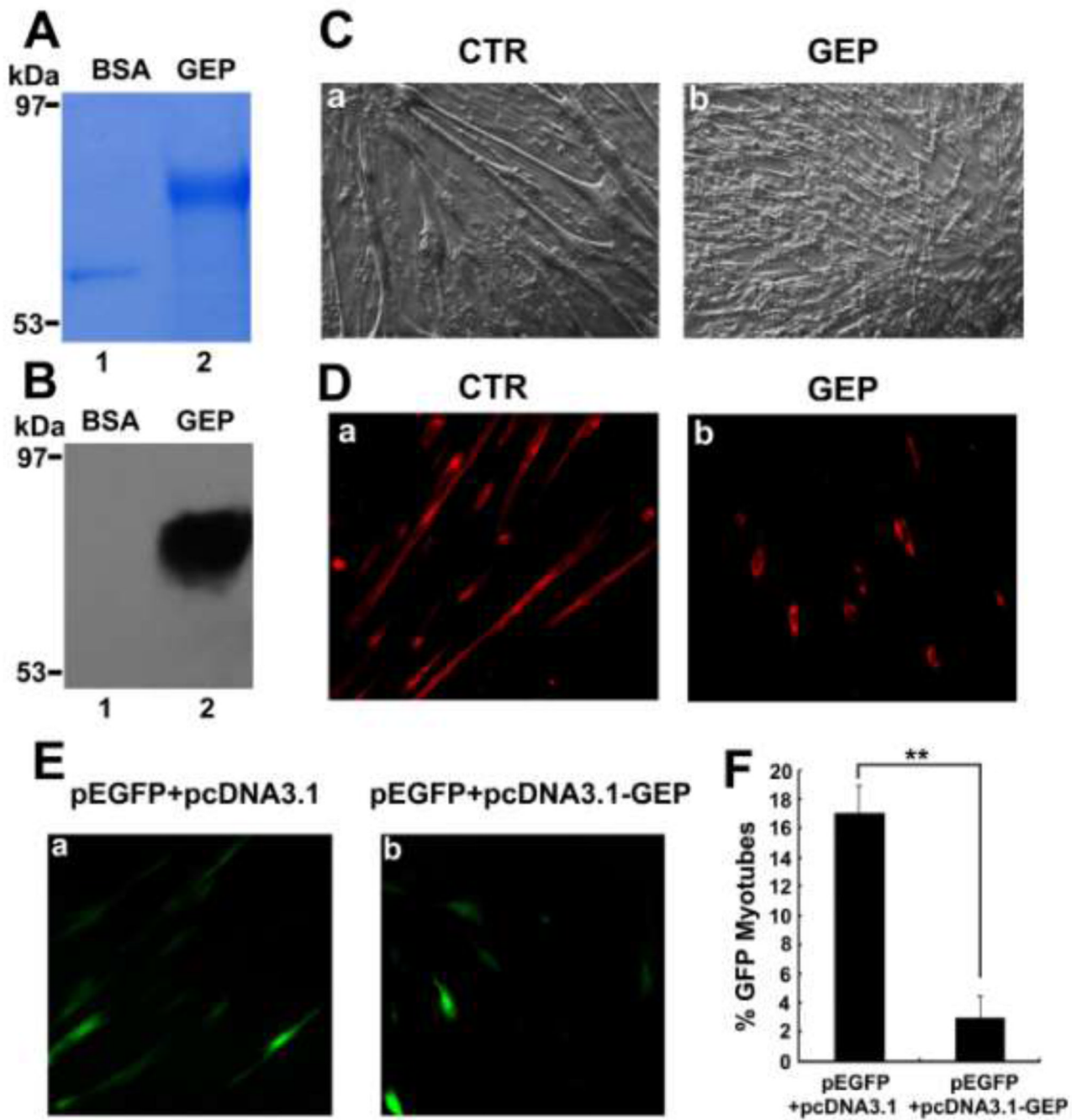


**FIGURE 4. GEP inhibits myogenic differentiation**

**Panel A-B. Purification of GEP.** The purified recombinant GEP protein was subjected to SDS-PAGE and examined by Coomassie Blue staining (Panel A) and Western blotting with anti-GEP antibodies (Panel B). **Panel C-D. GEP inhibits myotube formation in C2C12 cells.** C2C12 cells were cultured to confluency in GM. The cultures were then shifted to DM in the presence or absence of 100 ng/ml GEP for 5 days. The cultures were observed under a phase-contrast microscope (Panel C). After fixation and blocking, the cultures were stained with anti-MHC antibodies (Panel D). **Panel E-F. GEP overexpression inhibits myotube formation.** C2C12 myoblasts were transfected with pEGFP and pcDNA3.1 (1:20); or

pEGFP and pcDNA3.1-GEP (1:20). 24 h following transfection, cells were switched to DM for 5 days. Shown are representative images of GFP expressing cells under low magnification (Panel E). The mean number of myotubes expressing GFP was then quantified (Panel F) ( $n = 4$ ,  $**P < 0.01$ ).

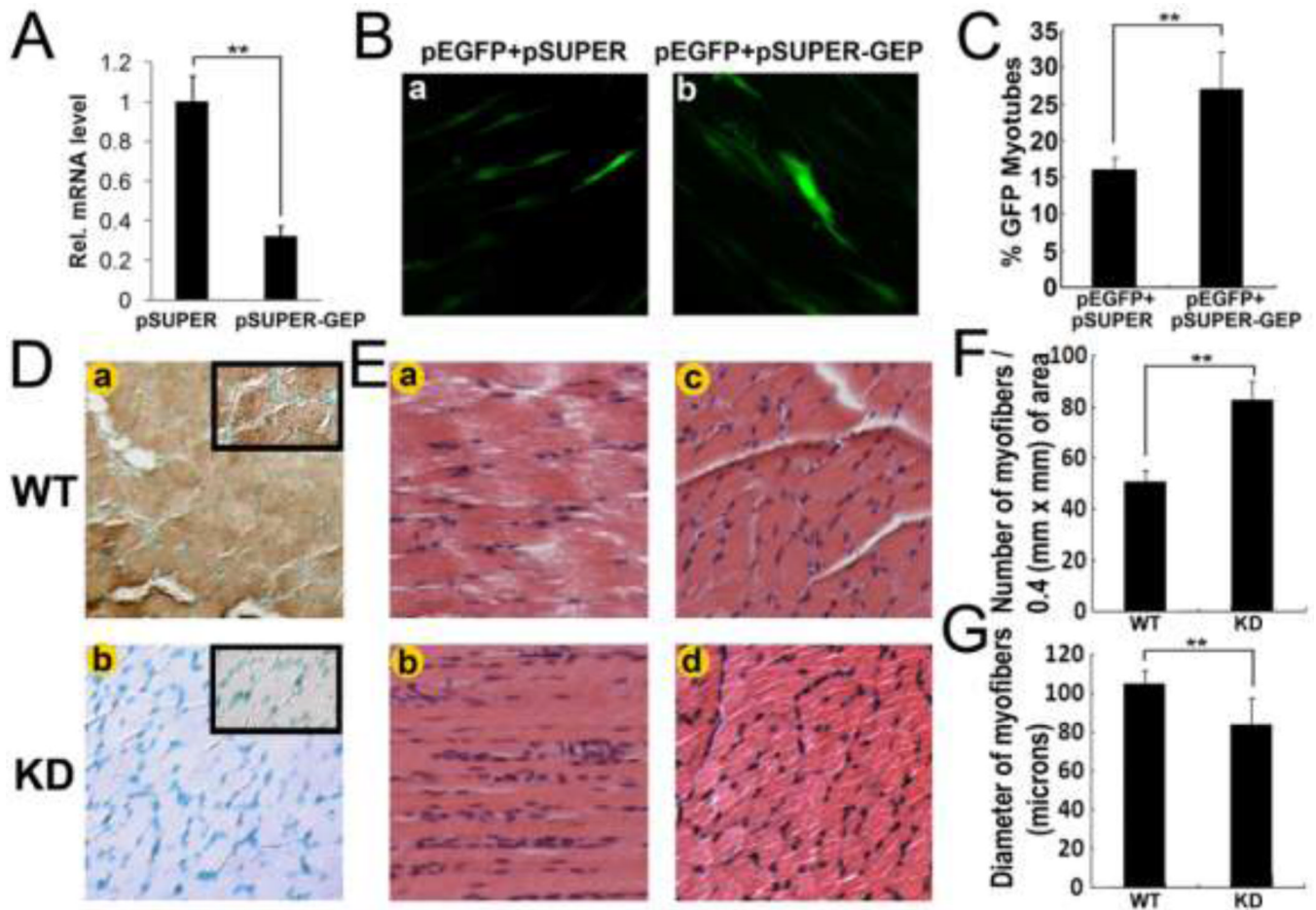


**FIGURE 5. Knockdown of GEP enhances myogenic differentiation**

**Panel A-C. GEP silencing enhances myotube formation.** In panel A, cells were transfected with either a siRNA-GEP expression plasmid pSuper-GEP or control vector pSuper and total RNA was collected for real-time RT-PCR. Expression of GEP was normalized against the GAPDH endogenous control. The normalized values were then calibrated against the control value, here set as 1,  $**p < 0.01$ . In panels B-C, C2C12 myoblasts in GM were transfected with either pEGFP and pSUPER (1:20) or pEGFP and pSUPER-GEP (1:20). 24 h following transfection, cells were switched to DM for 5 days. Shown are representative images of GFP expressing cells under low magnification. The mean percentage of myotubes expressing GFP was determined (Panel B) ( $n = 4$ ,  $**p < 0.01$ ).

**Panel D. GEP expression in the skeletal muscle from newborn wild type and *Grn* knockdown mice.** Muscle sections of WT (a) and *Grn* knockdown (b) mice were stained with anti-GEP antibodies (brown) and counterstained with Methyl green (green).

**Panel E. Myogenesis is enhanced in *Grn* knockdown mice.** Sections of quadriceps muscle from wildtype and *Grn* knockdown mice were stained with hematoxylin and eosin. Longitudinal sections of WT (a) and *Grn* knockdown (b) are shown alongside cross-sectional images of WT (c) and *Grn* knockdown (d).

**Panel F-G. Quantitative alternation in the number and size of the muscle fibers in *Grn* knockdown mice.** In Panel F, the number of myofibers / 0.4 (mm $\times$ mm) of area; in Panel G, the diameter of myofibers (microns). The measurement of the number and average diameters of myofibers was conducted with Northern Eclipse software (version 6.0, Empix Imaging Inc.).  $n=4$ .

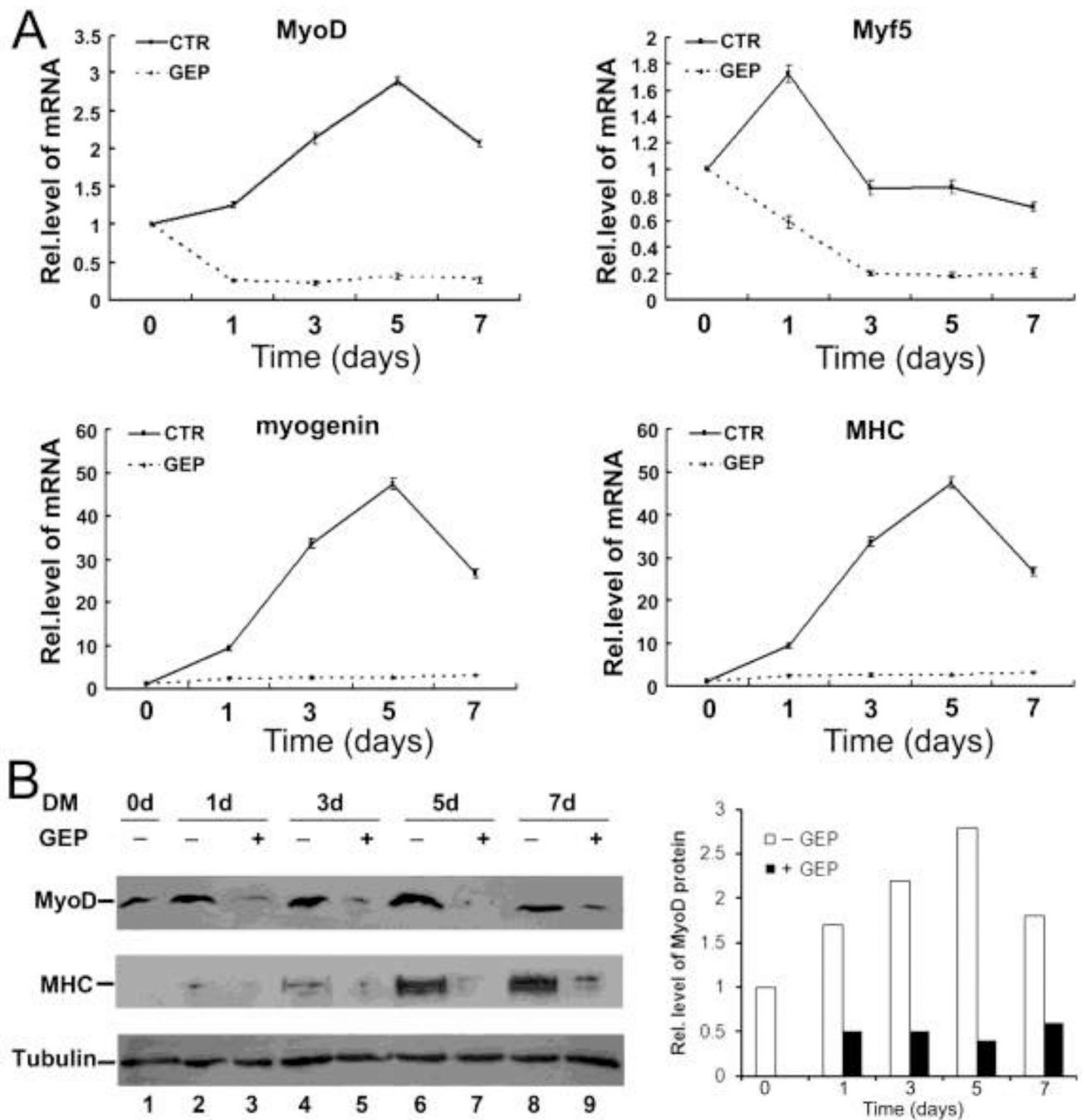


**FIGURE 6. GEP inhibits the expression of genes specific for myogenesis**

**Panel A. GEP inhibits MyoD, Myf5, Myogenin, and MHC mRNA expression.** C2C12 cells were cultured in GM to confluency and then shifted to DM in the presence or absence of 100 ng/ml GEP. Total RNA was extracted from cells at the indicated time points and the mRNA levels of MyoD, Myf5, Myogenin, MHC, and GAPDH were measured by real-time PCR. The expression of MyoD, Myogenin, Myf5, and MHC was normalized against GAPDH endogenous control. The units are arbitrary, and the relative level of mRNA on day 0 was set to 1. All experiments were repeated three times. Bar graphs show mean  $\pm$  SEM.

**Panel B. Left panel, GEP inhibits MyoD, Myf5, Myogenin, and MHC protein**

**expression in the course of myotube formation of C2C12 cells.** Total cell extracts obtained at the indicated time points were subjected to SDS-PAGE and Western blotting with anti-MyoD, anti-MHC, and anti-Tubulin (internal control) antibodies. **Right panel, Quantitative alternation in the MyoD protein level in response to GEP treatment during myotube formation.** The MyoD protein level in GEP-untreated C2C12 cells at day 0 time point was set at 1.

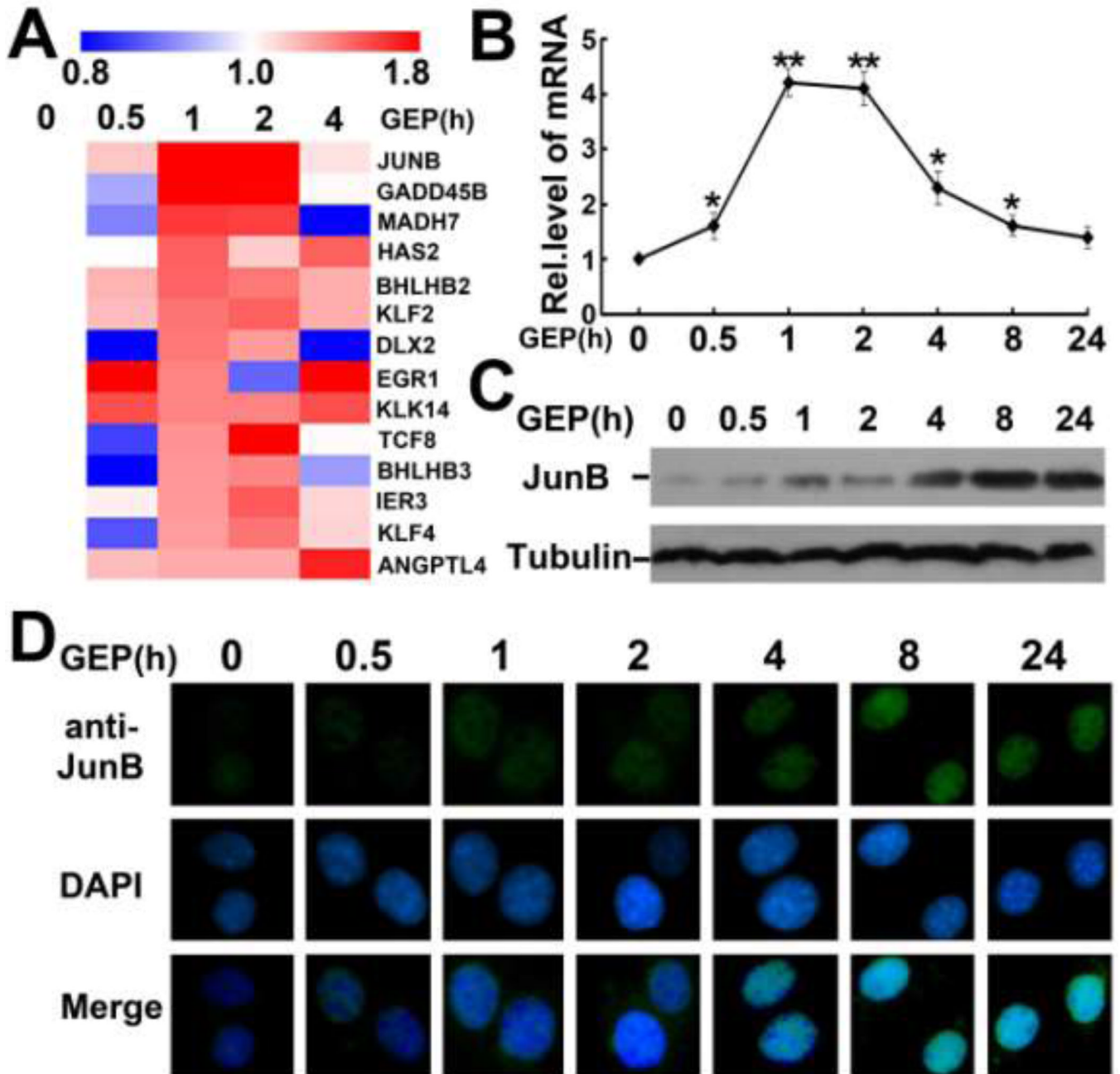


**FIGURE 7. JunB is a GEP-inducible gene**

**Panel A. Microarray gene expression analysis of C2C12 cells following GEP stimulation.** C2C12 cells were cultured in the presence of 100 ng/ml GEP. Cells were harvested at various time points and total RNA extracts were analyzed using microarray analysis. Assay was repeated and the genes showing reproducible changes were selected. Heatmap reflects gene expression values at several time points. Expression levels above 1.0 represent up-regulation, while those below 1.0 represent down-regulation. **Panel B. GEP induces JunB mRNA expression.** At various time points, total RNA extracts were isolated and subjected to real-time PCR. The graph shows the relative JunB mRNA level at the indicated time points. The units are arbitrary, and the relative level of JunB mRNA at hour 0

was set to 1. Experiments were repeated three times. Compared to the hour (h) 0 time point \*,  $P < 0.05$ ; \*\*,  $P < 0.01$ . **Panel C. GEP induces JunB protein expression.** At various time points, total cell extracts were isolated and subjected to Western blotting with anti-JunB and anti-Tubulin (internal control) antibodies. **Panel D. Immunofluorescence staining of GEP-induced JunB expression.** At various time points, the cells were fixed, blocked, and stained with anti-JunB (green). The nuclei were stained with 4, 6-diamidino-2-phenylindole (DAPI) (blue).

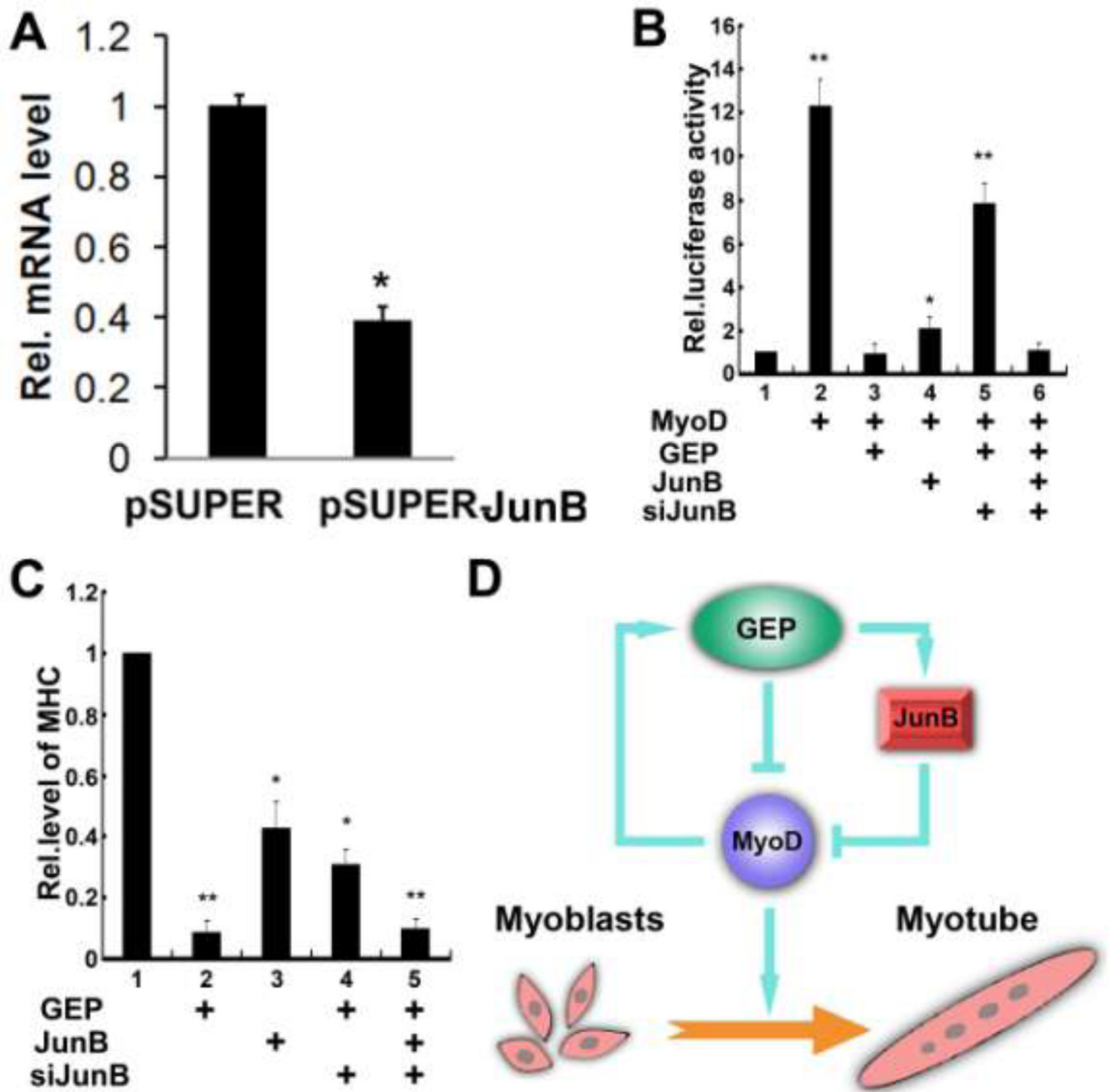


**FIGURE 8. GEP-mediated inhibition of MyoD activity depends on JunB**  
**Panel A & B. Silencing of JunB abolishes GEP-mediated inhibition of reporter gene activity.** In Panel A, cells were transfected with either pSuper-JunB or control vector pSuper, and total RNA was collected for real-time RT-PCR. The expression of JunB was normalized against the GAPDH endogenous control. The normalized values were then calibrated against the control value, here set as 1. \*\*,  $p < 0.01$ . In Panel B, C3H10T1/2 cells were co-transfected with p204-specific reporter plasmid pCMV-MyoD, pcDNA3.1-JunB, or pSuper-JunB, as indicated. The cells were cultured in the presence or absence GEP. 48 h following transfection, cells were harvested and luciferase and  $\beta$ -galactosidase activity were determined. Experiments were repeated three times. The relative luciferase activity of the

leftmost bar was set to 1. Compared to the leftmost bar \*,  $P < 0.05$ ; \*\*,  $P < 0.01$ . **Panel C. Silencing of JunB abolishes GEP-mediated inhibition of myogenesis.** C2C12 cells were transfected with pcDNA3.1-JunB and/or pSuper-JunB, as indicated. 24 h after transfection, the cells were shifted to DM and cultured with or without GEP. At day 5, total RNA was extracted and MHC expression levels were determined by real-time PCR, using GAPDH as an internal control. Experiments were repeated three times. The relative MHC expression level of the leftmost bar was set to 1. Compared to the leftmost bar \*,  $P < 0.05$ ; \*\*,  $P < 0.01$ . **Panel D. A proposed model for explaining the role and regulation of GEP in myogenesis.** MyoD induces the expression of GEP, whereas GEP inhibits myotube formation through either the direct inhibition of MyoD expression or the induction of JunB that in turn inhibits MyoD activity (7, 32). Thus, GEP, JunB, and MyoD constitute a regulatory feedback loop during myotube formation.